Article

4-Anilino-2-pyridylquinazolines and -pyrimidines as highly potent and non-toxic Inhibitors of Breast Cancer Resistance Protein (ABCG2)

Michael K Krapf, Jennifer Gallus, and Michael Wiese

J. Med. Chem., **Just Accepted Manuscript** • Publication Date (Web): 04 May 2017

4-Anilino-2-pyridylquinazolines and -pyrimidines as Highly Potent and Nontoxic Inhibitors of Breast Cancer Resistance Protein (ABCG2)

Michael K. Krapf, Jennifer Gallus, Michael Wiese*

Pharmaceutical Institute

University of Bonn

An der Immenburg 4

53121 Bonn, Germany

Keywords

ABC transporter; inhibitor; ABCG2; quinazolines

ABSTRACT

Multidrug resistance (MDR) mediated by ATP-binding cassette (ABC) transport proteins remains a major problem in the chemotherapeutic treatment of cancer and might be overcome by inhibition of the transporter. Due to the lack of understanding the complex mechanisms involved in the transport process, in particular for breast cancer resistance protein (BCRP/ABCG2), there is a persistent need for studies of inhibitors of ABCG2.

In this study we investigated a systematic series of 4-substituted-2-pyridylquinazolines in terms of their inhibitory potency as well as selectivity toward ABCG2. For comparison, the quinazoline scaffold was reduced to the significantly smaller 4-methylpyrimidine basic structure. Furthermore, the cytotoxicity and the ability to reverse MDR was tested with the chemotherapeutic agents SN-38 and mitoxantrone (MX). Interaction of the compounds with ABCG2 was investigated by a colorimetric ATPase assay. Enzyme kinetic studies were carried out with Hoechst 33342 as fluorescent dye and substrate of ABCG2 to elucidate the compounds binding modes.

Introduction

ATP-binding cassette (ABC) transporter form a large superfamily of which members are found in all organisms from bacteria over plants to men. In humans 49 ABC transporters and were identified and classified according to their phylogenetic similarities in seven subfamilies, ABC A to ABC G.[1,2,3] While most ABC transporters have well defined substrates, some are multispecific playing an important role in the protection of the human body against xenobiotics to enhance survival.[4] Naturally these are expressed in organs with barrier function, as intestine or the blood brain barrier. Unfortunately, they are frequently overexpressed in some tumor tissues which may lead to resistance against anticancer drugs and failure of a chemotherapeutic treatment due to insufficient drug concentration in the cancer cell.[5] Regarding dissemination of tumors, chemotherapy remains the most promising therapy although its prognosis of curing is rather limited due to acquired or intrinsic drug resistance which accounts for roughly 90% of treatment failures.[6] This so called multidrug resistance (MDR) is often associated with the three major MDR related ABC transport proteins, P-glycoprotein (P-gp, ABCB1), multidrug resistance-associated protein 1 (MRP1, ABCC1) and breast cancer resistance protein (BCRP, ABCG2).[7,8] Among these, ABCG2 was most recently discovered and found to be mainly overexpressed in drug-resistant solid tumors as well as hematopoietic tumors.[9,10]

Unlike ABCB1 and ABCC1, the breast cancer resistance protein ABCG2 is a half-transporter consisting of 655 amino acids with only one cytosolic nucleotide-binding domain (NBD) and one transmembrane domain (TMD).[8] For its function it is assumed to form dimers or tetramers as several studies suggest.[11, 12, 13] Also, the details of the transport process of the drugs remain unclear and there is need for further investigations.[14, 15]

Recently, a crystal structure of the human sterol transporter ABCG5/ABCG8 was published that could be used for homology modeling of ABCG2.[16] Although the X-ray crystal structure of the protein possessed a relative low resolution of 3.9 Å only it is the first structure with an inverse organization of the NBD and TMD domains. Shortly afterwards a homology model of ABCG2 was created and employed to investigate substrate binding, and effects of point mutations in the transporter comparing the *in silico* results to experimental data.[17]

Since its discovery in 1998 by Doyle et al. in MCF-7/AdrVp human breast cell carcinoma cells, many chemotherapeutics like mitoxantrone (MX), flavopiridol, methotrexate, irinotecan and its active metabolite SN-38 were identified as substrates of ABCG2.[18,1] Therefore, inhibition of the target with potent, selective and nontoxic inhibitors in co-administration could be a possible approach to overcome ABCG2 caused MDR.[19, 20] Recent studies suggest, that the expression of ABCG2 in colorectal cancer is associated with shortened patient survival and less response to chemotherapeutic treatment with oxaliplatin and 5-fluorouracil (FOLFOX).[21, 22] Although ABCG2 expression and clinical outcomes sometimes found to be contradictory, inhibition of ABCG2 remains a promising tool to increase the oral bioavailability of chemotherapeutics or to overcome MDR.[19]

Relating to inhibitors of ABCG2, only a few potent compounds active at a submicromolar concentration range have been reported, revealing high selectivity and low cytotoxicity.[23] As one of the first potent inhibitors, fumitremorgin C (FTC) was isolated from *Aspergillus fumigates* and found to restore sensitivity toward MX in the resistant S1-M1-3.2 cell line.[24,19] Due to neurotoxic effects of FTC, an analog named Ko143 (**55**) was developed.[25] This second generation inhibitor exhibited moderate toxicity and a high inhibitory potency as well as good selectivity toward ABCG2. However, recent studies suggest that selectivity at concentrations $\geq$ 1 μM is restricted, since effects on the transport activity of ABCB1 and ABCC1 were observed.[26] Recently the synthesis of highly potent and nontoxic inhibitors with a phenolic indeno[1,2-b]indole core has been reported.[27] And more recently highly potent and nontoxic

inhibitors containing the chromone scaffold with potency comparable to compound **55** have been developed by the same working group.[28] Also tyrosine kinase inhibitors like gefitinib that found clinical application in the treatment of cancer have been shown to be potent inhibitors of ABCG2.[29]

Based on the quinazoline scaffold of gefitinib, we designed a focused library of different 4-substituted-2-phenylquinazolines. The studies revealed distinct trends regarding different substitutions and yielded new compounds, some with higher inhibitory potencies than compound **55** as well as high selectivity toward ABCG2 and considerable low toxicities.[30, 31, 32] In the present study, a pyridyl substituent was introduced in position 2 with the nitrogen in *ortho*, *meta* and *para* position. Additionally, a systematic variation at the anilino linker in position 4 was carried out in *meta* and *para* position to elucidate the structure-activity relationship (SAR) providing a comparison to the 2-phenyl analogs from our previous study.[32] Moreover, compounds based on a 4-methylpyrimidine scaffold were synthesized to investigate the importance of the condensed aromatic ring of the quinazoline scaffold with regard to its inhibitory potency toward ABCG2.

On the basis of the new findings, insights in the development of new potent inhibitors based on both, a quinazoline and a 4-methylpyrimidine scaffold is provided, yielding new inhibitors of ABCG2 with promising characteristics for further *in vitro* and *in vivo* applications.

Results and Discussion

Chemistry. A brief description of the synthetic route for all compounds is provided in Scheme 1. Precursors of the quinazoline derivatives were prepared by a cyclic condensation reaction of anthranilamide with the corresponding pyridine carboxaldehyde to yield the 2-substituted quinazolinone derivatives **1-3**. Chlorination of position 4 of the quinazolinone derivative was achieved by refluxing with $POCl_3$ to obtain the 4-chloro derivatives **4-6**. Final

compounds **11-41** were synthesized by aromatic nucleophilic substitution of **4-6** with a *meta* and/or *para* substituted aniline derivative using microwave irradiation.

The 2-substituted 6-methyl-pyrimidine derivatives **42-48** were synthesized starting from a cyclic condensation reaction of methyl 3-oxobutanoate with isonicotinimidamide or benzimidamide to obtain **7** and **8**, respectively. Refluxing with $POCl_3$ yielded the 4-chloro derivatives **9** and **10**. In the last step the chloro-substituted compounds were reacted with a *meta* and/or *para* substituted aniline derivatives using microwave irradiation to yield **42-48** by a nucleophilic aromatic substitution reaction.

Since *ortho*-substitution of the 4-anilino linker resulted in poor inhibitory activities in previous studies, only *meta* and *para* substitutions were considered in this work.

The identity of all compounds was confirmed by ^{1}H and ^{13}C NMR spectra and the purity by elemental analysis. Moreover, the melting points of all test compounds were determined.

Biological Evaluation.

Hoechst 33342 Accumulation Assay. The Hoechst 33342 accumulation assay was used to determine the inhibitory activity of each test compound against ABCG2 using the MDCK II BCRP cell line. The fluorescent dye Hoechst 33342 is a substrate of ABCG2 and significantly increases its fluorescence when bound to DNA or embedded in lipophilic environment like the cell membrane. [33] This is utilized to determine the intracellular accumulation of the substrate that correlates with the degree of inhibition of the transport protein by a compound.

An overview of the inhibitory activities obtained in the Hoechst 33342 accumulation assay along with the structural features of the compounds is depicted in Table 1. A summary of the SAR is given in the end of this section providing a quick overview of the most important results (Figure 2).

At first, the interrelation of the *ortho*, *meta* and *para* substituted pyridyl residue on position 2 (R^1) with differently substituted 4-anilino residues (R^2) was investigated for the quinazoline

scaffold A: compounds **11**, **12** and **13** all contain a 3-nitro substitution at R^2 whereas R^1 is equipped with an *ortho*, *meta* or *para* substituted pyridyl residue, respectively. Inhibitory activities against ABCG2 expressed by the IC_{50} values of 376 nM, 105 nM and 117 nM were obtained in the given order of the compounds. Interestingly, the *ortho* pyridyl substitution on R^1 yields approximately a three-fold decreased inhibitory activity in comparison to the *meta* and *para* analogs. Similar observations were made for the next series with a 3-cyano residue at R^2: again the *ortho* pyridyl species **15** showed a significantly lower activity (IC_{50}: 507 nM) than its *meta* and *para* analogs **16** (108 nM) and **17** (134 nM), respectively. For derivatives with a 3-methoxy group at R^2 the same trend was observed with regard to the pyridyl group at R^1: compound **19** with the 2-pyridyl substitution was the least potent (1630 nM), while *meta* and *para* pyridyl derivatives yielded lower IC_{50} values of 1020 nM (**20**) and 558 nM (**21**), respectively. This clearly illustrates that an *ortho* pyridyl residue at R^1 decreased the inhibitory activity against ABCG2 in every derivative tested so far. Therefore we concentrated our efforts on compounds with *meta* and *para* pyridyl groups.

Compound **14** with a 3-pyridyl residue at R^1 and a 4-nitro substituent at R^2 yielded the lowest IC_{50} value in the test set (64.1 nM) and confirmed the results of previous studies that *meta* and *para* substitutions at the anilino moiety (R^2) with nitro, cyano, trifluoromethyl and other residues is beneficial for high inhibitory activities.[30, 32] In comparison to the standard inhibitor **55** (IC_{50}: 227 nM in the Hoechst 33342 accumulation assay), currently one of the most potent inhibitors of ABCG2, compound **14** is roughly four-fold more potent.

In most cases a *meta* substitution at R^2 resulted in higher inhibitory potency than the corresponding *para* substituted derivative. The differences varied from slight 3-methoxy (**21**, IC_{50}: 558 nM) and 4-methoxy (**22**, IC_{50}: 742 nM) to more than two-fold (compounds **26**, IC_{50}: 216nM; **27**, IC_{50}: 488 nM). But there were significant exceptions where the para substituted derivative was more potent. Compare compounds **12** and **14**, or **49** and **50**. Due to the fact that further enhancement of the inhibitory activity was often achieved by disubstitution of the

anilino moiety R^2 at positions 3 and 4 of a 2-phenylquinazoline scaffold,[30, 32] several combinations were investigated.

The 3,4-dimethoxy substituted compound was investigated with different pyridyl residues at R^1. Again the *ortho* pyridyl derivative **23** was least potent with an IC_{50} of 1060 nM, while the *meta* and *para* derivatives yielded lower IC_{50} values of 753 nM and 545 nM, respectively. Disubstitution led to a slight potency increase compared to the mono-methoxy derivatives.

The combination of a 3-trifluoromethyl and 4-methoxy group at R^2 along with a 4-pyridyl residue at R^1 as present in compound **28** resulted in an IC_{50} of 146 nM which exceeded the inhibitory potency of both single substitutions found in compounds **22** and **26.** In the following, the effect of substituents with strong influence on the electron density of the aromatic residue R^2 was investigated using a strong electron withdrawing group and a strong electron donating group. Hence, compound **30** with a 3-fluorosulfonyl residue at R^2 and 4-pyridyl at R^1 was compared with **31**, comprising a 3-dimethylamino group at R^2 and 3-pyridyl at R^1. Both compounds yielded increased IC_{50} values of 1380 nM and 1200 nM, respectively. This is in agreement with earlier results confirming that the electron density at the anilino moiety does not play a major role for the inhibitory activity of a compound. Furthermore a more bulky ester was synthesized to elucidate some more structure activity relations. Hence, a *tert*-butyl 3-aminobenzoate residue at position 4 was combined with a 4-pyridyl residue at R^1 (**39**). The obtained IC_{50} of 299 nM is negligibly lower than the value found for the methyl ester analog **38**. Compounds containing an ionized carboxy group possessed the lowest inhibitory activities in the test set with IC_{50} values in the micromolar range.

Although the IC_{50} values of the *meta* and *para* substituted 2-pyridylquinazoline derivatives were so far in good agreement with the IC_{50} values in the 2-phenylquinazoline series, a 3-fluoro residue at R^2 with a 3-pyridyl moiety at R^1 (**29**) resulted in a much lower IC_{50} of 156 nM than its phenyl analog **53** (363 nM). With regard to substitution of phenyl or *para* pyridyl at R^1, the largest differences were observed for a hydroxy substitutent at R^2. Compound **32**

with a 3-hydroxy group at R^2 and 4-pyridyl at R^1 yielded an IC_{50} of 1070 nM and the corresponding 4-hydroxy derivative **33** yielded an IC_{50} of only 4260 nM. While for the 2-phenylquinazoline analog **52** with 4-hydroxy at R^2 an excellent IC_{50} of 211 nM had been found. Furthermore, a 3-hydroxymethyl group at R^2 was either combined with 3-pyridyl (**34:** 810 nM) or 4-pyridyl (**35:** 921 nM) at R^1. The alteration from 3-hydroxy to 3-hydroxymethyl had only slight effects on the inhibitory activity. Again, no significant distinction between *meta* and *para* pyridyl was observed regarding the inhibitory activity. Following, a disubstitution of 3-hydroxy and 4-nitro at R^2 was investigated with a 3-pyridyl moiety on R^1. The resulting IC_{50} value of 245 nM for compound **36** was about three-fold higher than for the 2-phenylquinazoline analog **51** (IC_{50}: 81.1 nM). This is probably due to unfavourable effects of the 3-pyridyl group at R^1 which results in lower inhibitory activities when combined with *meta* or *para* hydroxy residues at R^2 as observed in case of compounds **32** and **33**.

In the next series, the condensed aromatic ring next to the heterocycle of the quinazoline scaffold was replaced by a methyl group (Table 1, scaffold **B**) to evaluate the impact of the aromatic moiety on the inhibitory activity. For better comparison a 4-pyridyl as well as a phenyl residue was investigated at R^1 to give insights in the SAR of these small molecules. First, a 4-pyridyl residue at R^1 and a 3-cyano group at R^2 were introduced in compound **42**. The resulting IC_{50} of 132 nM is in excellent agreement with its quinazoline analog **17** (IC_{50}: 134 nM). Furthermore, compounds **43** and **44** with a 4-pyridyl residue at R^1 together with a 3-methoxy or 4-methoxy group at R^2 yielded IC_{50} values of 271 nM and 874 nM. In accordance to the *meta* and *para* methoxy substituted quinazoline analogs **21** (IC_{50}: 558 nM) and **22** (IC_{50}: 742 nM) the *meta* substitution resulted in higher inhibitory potency. Moreover, some 4-methylpyrimidines bearing a 2-phenyl group were investigated. Two derivatives with *meta* or *para* cyano substituents at R^2 yielded IC_{50} values of 122 nM (**45**) and 128 nM (**46**), respectively. Both values are in good agreement with their 2-phenylquinazoline analogs with a 3-cyano (**49**: 140 nM) or a 4-cyano (**50**: 71.4 nM) residue at R^2. Also, the disubstitution with

3-nitro and 4-hydroxy at R^2 exhibited only negligible differences between the 2-phenyl derivatives of scaffold B (**47**: 98.8 nM) and scaffold A (**51**: 81.1 nM). For the basic structures of scaffold A and scaffold B with R^1 = phenyl and R^2 = H, very similar IC_{50} values of 648 nM (**48**) and 882 nM (**54**) were found. Concentration-response curves of the two most potent compounds **14** and **47** in comparison to the standard inhibitor **55** are depicted in Figure 1.

From this study it was found that the substitution pattern of the pyridyl residue at R^1 of scaffold A has a major impact on the inhibitory activity: substitution with *ortho* pyridyl yielded less potent compounds while *meta* and *para* substitutions both resulted in increased activities. Regarding the substituents at R^2, nitro, cyano, trifluoromethyl or fluoro substituents in *meta* and *para* yielded very potent inhibitors. No clear preference was noticeable for *meta* and *para* substitution of compounds containing a pyridyl or phenyl moiety at R^1. In contrast to earlier studies, hydroxyl residues turned out to decrease the inhibitory activity when combined with pyridyl at R^1 instead of phenyl.[32] Apart from that, very similar potencies were obtained with both moieties. Again, the electron density of the aromatic ring influenced by substituents at R^2 exhibits no clear correlation with the IC_{50} values. Introducing esters in *meta* position also resulted in high activities independent of the bulkiness of the alkyl residue. According to calculation, the pyridyl residue decreases the logP in comparison to a phenyl substitution by about 1.18 units to an average of 3.00. No correlation of the calculated logP values with the pIC_{50} values was observed.

Interestingly, the potency of the 4-methylpyrimidine analogs, lacking the condensed aromatic ring of the quinazoline scaffold, was similar to the quinazoline based derivatives. Earlier studies have emphasized the need of aromatic substitution at R^1 as well as the importance of the nitrogen in position 3 of the heterocycle for potent compounds.[30, 32] Simplification of the quinazoline scaffold to a 4-methylpyrimidine heterocycle leads to an extraordinary high

ligand efficacy, reducing relevant components for a potent inhibitor to three aromatic rings substituted with few small residues.

Screening for ABCB1 and ABCC1 Inhibition. The selectivity of selected compounds toward ABCG2 was investigated by the calcein AM assay. For this purpose, the ABCC1 overexpressing cell line H69AR and the ABCB1 overexpressing cell line A2780adr were used as described in the experimental section. A screening of the inhibitory effect of the substances toward the polyspecific transporters ABCB1 and ABCC1 was carried out at a concentration of 10 μM. Cyclosporine A (CsA) was used as positive control, leading to total inhibition of both transporters. Compounds which exhibit an inhibitory potency of more than 25% relative to the standard were additionally tested with more dilutions to generate a concentration-response curve to calculate an IC_{50} value. The screening results for the inhibitory activity toward ABCB1 and ABCC1 are depicted in the bar charts Figure 3 (a) and (b), respectively. A summary of the IC_{50} values of the compounds showing more than 25% of inhibition in the screening is given in Table 2.

In the calcein AM assay with ABCB1 overexpressing cells, the following compounds showed a relative inhibitory activity of more than 25% in relation to the positive control CsA. Bearing a 3-methoxy residue at R^2, compounds **19**, **20** and **21** show relatively high inhibitory activity toward ABCB1. They were synthesized in the given order with a *ortho*, *meta* and *para* pyridyl moiety at R^1 and have IC_{50} values of 12.7 μM, 4.78 μM and 5.43 μM, respectively. As expected, the inhibitory activity toward ABCB1 is increased for the 3,4-dimethoxy derivatives, since methoxy groups are favourable for ABCB1 inhibition.[32] The *ortho*, *meta* and *para* pyridyl (R^1) substituted compounds **23**, **24** and **25** show inhibitory activities of 6.30 μM, 3.11 μM and 2.08 μM, respectively. As observed for inhibition of ABCG2, the substitution pattern of the pyridyl residue is also crucial for the inhibitory potency against ABCB1. Substitution with *ortho* pyridyl decreases the activity in comparison to the *meta* and

para derivatives. In comparison to the mono-substituted compound **22**, **28** revealed a good IC_{50} value of 2.78 μM with 4-pyridyl at R^1 and a disubstitution with 3-trifluoromethyl and 4-methoxy at R^2. Furthermore, a 4-pyridyl residue at R^1 combined with a methyl 3-aminobenzoate moiety (**38**: IC_{50} = 6.37 μM) or a *tert*-butyl 3-aminobenzoate residue (**39**: IC_{50} = 0.334 μM) at position 4, led to noticeable inhibition of ABCB1. In particular, the *tert*-butyl ester obtained a considerable potency superior to the standard CsA (IC_{50}: 1.21 μM). A concentration response curve of **39** and CsA is provided in Figure 4. Then, a substitution of 4-pyridyl at R^1 each with a 3-aminobenzoic acid (**40)** and a 4-aminobenzoic acid moiety (**41**: IC_{50} = 3.67 μM) was carried out. The *meta* substituted compound exhibited no activity whereas the *para* substituted one possessed a considerable potency.

All of the investigated nitro and cyano substituted compounds **11**-**18** showed high activities toward ABCG2 and low activities toward ABCB1. Compounds bearing at least one methoxy group generally showed an increased inhibitory activity toward ABCB1. Adding more methoxy groups to the molecule resulted in a further increased activity. Additionally, a correlation of the substitution pattern of the pyridyl residue at R^1 was observed, showing increased activities from *ortho* to *meta* to *para*. Some ester moieties also exhibit significant potencies in the screening: compound **39** with a *tert*-butyl ester had the lowest IC_{50} value of 0.334 μM.

To investigate the inhibitory effect of the compounds toward ABCC1, they were screened in a calcein AM assay with the ABCC1 overexpressing cell line H69 AR. The results of the screening are depicted in Figure 3 (b) as a bar chart. Only compounds **22** and **47** slightly exceeded the 25% range of inhibitory activity relative to the positive control CsA (IC_{50}: 2.97 μM) at a concentration of 10 μM. It was found in earlier studies that compounds with a quinazoline scaffold, like the substituted 4-anilino-2-phenylquinazolines, exhibit no inhibitory activity toward ABCC1 unless they form charged species under physiological conditions.[32]

Compound **22** (IC_{50}: 15.9 μM) was the only one from the quinazoline series that slightly exceeded the 25% mark.

For the substances with a 4-methyl pyrimidine structure (scaffold B), only a negligible activity was found. Mere compound **47** (IC_{50}: 17.8 μM) with a disubstitution of 3-nitro and 4-hydroxy at the aniline moiety showed barely more than 25% of inhibition compared to the positive control CsA. Regarding quinazoline derivatives as inhibitors of ABCC1, this study is consistent with earlier findings, that inhibitory activity toward ABCC1 plays only a negligible role. [30, 32]

Determination of the Intrinsic Cytotoxicity via MTT Assay. The intrinsic cytotoxicity of selected compounds was determined in the MTT assay. The results for selected compounds are depicted in Table 3 and given as cell growth inhibition leading to a cell survival of 50% of the control (GI_{50}). Small amounts of methanol (1.8%) and DMSO (1%) from the stock solutions of the compounds were present at the highest concentration of 100 μM leading to apparent slight toxicity of otherwise nontoxic compounds. Therefore, additionally, the toxic effect of the used dilution without modulator was determined at GI_{50} = 96.1 μM (MDCK II ABCG2 overexpressing cells). For comparison, the GI_{50} of the established inhibitor of ABCG2 compound **55** (12.6 μM) was obtained in analogy to the other test substances.

Four potent compounds (**14**, **16**, **17** and **47)** with low intrinsic cytotoxicity were additionally investigated in a modified MTT viability assay without DMSO and with a constant amount of 1% methanol. This modification was possible due to the good water solubility of the compounds. Either no effect or stimulation of the cell proliferation was observed at low concentrations which is probably explained by a defensive cellular mechanism. Further increase of the concentration eventually reversed this effect leading to a decreasing cell viability.

All tested compounds showed no significant cytotoxic effects up to 100 μM. Due to restricted solubility, higher concentrations could not be used in order to create sigmoidal dose-viability curves obtaining a GI_{50} value. Thus, the GI_{50} of the nontoxic compounds is very likely higher than 96 μM, resulting from the cytotoxic effects of the solvents only.

The following section discusses GI_{50} values determined with the MTT assay using MDCK II ABCG2 overexpressing cells.

For the 3-nitro (**12**) and 4-nitro (**14**) substituted compounds (R^2), both with a 3-pyridyl moiety at R^1, GI_{50} values of 70.8 μM and 73.3 μM were calculated, respectively, revealing almost no cytotoxic effect caused by the compounds. Moreover, a compound containing 3-cyano residue at R^2 was investigated with a *meta* pyridyl (**16**) and *para* pyridyl (**17**) residue at R^1. Here, both compounds show very low cytotoxicity of 75.3 μM and 88.1 μM, respectively. Furthermore, the 3-pyridyl (R^1), 4-cyano (R^2) derivative **18** was investigated. Again, only negligible cytotoxicity was found giving a GI_{50} of 79.4 μM. By the first results some trends among the nitro and cyano substituents at R^2 combined with *meta* and *para* pyridyl moieties at R^1 can be perceived: substitution with cyano resulted in slightly decreased toxic effects in comparison to nitro, although both yielded considerably high GI_{50} values. Moreover, substitution with *meta* pyridyl seems to be beneficial for low cytotoxicity over a *para* substitution based on compounds **16** and **17**. Although the differences among the pyridyl derivatives are rather small, the advantage of the pyridyl over a phenyl moiety becomes clearly evident by comparison of compounds **18** and **49**. Both contain a 4-cyano substitution at R^2 along with 3-pyridyl or a phenyl residue at R^1, respectively. The phenyl derivative **49** has approximately an 8-fold lower GI_{50} (10.4 μM) than the 3-pyridyl derivative **18** (GI_{50}: 79.4 μM). This observation was also made for several more compounds presented below. Another effect was noticed regarding the substitution in *meta* and *para* position: the 4-pyridyl (R^1) derivatives substituted with trifluoromethyl groups in *meta* (**26**) or *para* (**27**) position resulted in GI_{50} values of 12.6 μM and 117 μM what reflects the great impact of this modification

(*meta* vs. *para*), which is also noticeable by the significant difference of the compounds IC_{50} values. Similar results were also found in earlier studies with the 2-phenyl analogs regarding the IC_{50} values and particularly the GI_{50} values.[32] A possible explanation for this observation was suggested by studies of the enzyme kinetics and ATPase assays described in the corresponding chapters. The lowest GI_{50} value (2.88 μM) in the test set was obtained for compound **28** with a 4-pyridyl residue at R^1 and a disubstitution of 3-fluoromethyl and 4-methoxy at the aniline moiety in position 4. In comparison to compound **26**, the additional methoxy group lowers the GI_{50} about four-fold. Compound **29** with a 3-pyridyl moiety at R^1 and 3-fluoro at R^2 has a GI_{50} of 46.8 μM. The comparison to its 2-phenyl analog **53** (GI_{50}: 18.0 μM) once more demonstrates the beneficial effect of the pyridyl moieties for cytotoxicity. Compound **31** with a 3-pyridyl moiety (R^1) and a 3-dimethylamino group (R^2) shows an increased cytotoxicity (GI_{50}: 10.0 μM). Furthermore, a 4-pyridyl substitution at R^1 was combined with 3-hydroxy (**32**) and 4-hydroxy residue (**33**) at R^2, respectively. The *meta* substitution was found to be considerably more cytotoxic (GI_{50}: 9.22 μM) than the *para* derivative (GI_{50}: 55.0 μM). Similar tendencies regarding IC_{50} and GI_{50} values as found for compounds **26** and **27** apply for the *meta* and *para* hydroxy derivatives. As expected, the 2-phenyl analog **52** exhibits a significantly higher cytotoxicity than compound **33** with a pyridyl moiety.

Additionally, some derivatives with the pyrimidine scaffold B were investigated. First, compound **42** containing a 4-pyridyl substituent at R^1 and a 3-cyano group at R^2. The determined GI_{50} of 6.92 μM discloses a considerably higher cytotoxicity than its quinazoline analog **17** (GI_{50}: 88.1 μM). Moreover, compound **46** with a phenyl substitution at R^1 along with a 4-cyano group at R^2 was investigated yielding a GI_{50} value of 17.8 μM which is slightly less toxic than the corresponding quinazoline analog **49** (GI_{50}: 10.4 μM). Further, compound **47** with a phenyl residue at R^1 and a disubstitution of 3-nitro and 4-hydroxy at R^2 had a GI_{50} of 49.0 μM which is identical to the quinazoline analog **51** (GI_{50}: 52.4). Due to the

low cytotoxicity along with the observed high inhibitory activity, high therapeutic ratios were obtained for such combinations (see Table 3). Finally, the basic scaffold B bearing phenyl at R^1 and hydrogen at R^2 was investigated: the calculated GI_{50} of 107 μM for compound **48** was significantly higher than for its analog derivative **54** based on scaffold A (GI_{50} = 26.6 μM).

From the data it can be concluded, that *meta* and *para* pyridyl residues (R^1) on a quinazoline scaffold A reduce the cytotoxicity in comparison to a phenyl moiety considerably. For the *meta* and *para* substitutions at R^2 distinct differences were observed concerning the GI_{50} as well as IC_{50} values. In general the 2-phenyl derivatives based on a 4-methylpyrimidine scaffold B exhibit a lower cytotoxicity in comparison with their quinazoline analogs based on scaffold A. However, scaffold B was less beneficial in comparison to scaffold A with a 4-pyridyl residue at R^1 and 3-cyano at R^2 (see **17** and **42**). Due to the limited amount of investigated compounds containing scaffold B in the MTT toxicity assay, further compounds have to be synthesized and investigated to confirm these findings.

Determination of the Ability to Reverse MDR via MTT Assay. A MDR reversal assay was performed for some of the most active compounds (**14**, **16** and **47**). The assay was carried out with MDCK II ABCG2 overexpressing cells. As a cytostatic drug, SN-38, which is a well-known substrate of ABCG2, was used. Different dilutions of the cytostatic were combined with different modulator concentrations. Intracellular accumulation of the cytostatic is induced by the inhibitory effect of the modulator toward ABCG2, which restrains the efflux of SN-38 out of the cell and leads to a decreased cell viability. As a positive control the MDCK II parental cells were used to represent total inhibition due to the lack of ABCG2 transport proteins. The evaluation of the assay was carried out analogously to the MTT viability assay described above.

For this investigation, the most potent 2-pyridylquinazoline derivatives containing a nitro (**14**) and a cyano (**16**) group were selected. Additionally, compound **47** was chosen from the derivatives based on the 4-methylpyrimidine scaffold B due to its highest inhibitory activity among them. All compounds displayed the ability to fully reverse the MDR of the ABCG2 overexpressing cells, as shown in Figure 7 (a, c and e). Reversal of the resistance is illustrated by the shift of the IC_{50} values of the ABCG2 overexpressing cells toward the parental cells with increasing modulator concentration (grey arrow). At a modulator concentration of ≥ 1 μM full sensitization of the ABCG2 overexpressing cells was achieved, indicated by a similar IC_{50} value as the parental cells. Additionally, the MTT assay was repeated using parental MDCK II cells to elucidate possible interactions of the modulator and SN-38 which could affect the IC_{50} values obtained from the concentration-response curves. The obtained concentration-response curves are shown in Figure 7 (b, d and f). Clearly, there is no effect of the compounds on the wild type cells. Furthermore, a quantification of a compounds efficacy in reversing MDR was calculated by plotting each GI_{50} value from the reversal assay against the logarithm of the compound concentration and calculating an IC_{50} value: the state "no inhibition" is defined with ABCG2 overexpressing cells without modulator, which show maximal resistance toward SN-38, and "total inhibition" of ABCG2 is defined by the pIC_{50}-value of the parental cells. Corresponding concentration-response curves were fitted with the logistic equation yielding pEC_{50} values that can be compared with the inhibitory activities from the Hoechst 33342 accumulation assay (Figure 8).

Compound **14** with a 3-pyridyl residue at R^1 and a 4-nitro group at R^2 (scaffold A) yielded an EC_{50} of 21.2 nM determined in the MDR reversal assay. This suggests an about 3-fold higher inhibitory potency for inhibiting the transport of SN-38 than found in the Hoechst 33342 accumulation assay (64.1 nM). As expected, the compound obtained a sigmoidal curve with the ABCG2 overexpressing cells (●) and reaches its top on a similar level to the parental cells (○) with increasing modulator concentration (Figure 8 a). Moreover, the IC_{50} values of the

parental cells stay the same throughout the different modulator concentrations. Following, for compound **16** with a 3-pyridyl moiety at R^1 and 3-cyano at R^2 (scaffold A) an IC_{50} value of 85 nM was calculated with this method (Figure 8 b). This is again slightly less than the IC_{50} value of 108 nM found in the Hoechst 33342 accumulation assay. Also compound **47** with a phenyl moiety at R^1 and a disubstitution of 3-nitro and 4-hydroxy at R^2 (scaffold B) exhibits a good correlation of the IC_{50} value derived from the MDR reversal assay (62.3 nM) and the Hoechst 33342 accumulation assay (98.8 nM). The differences in the IC_{50} values can be explained by different affinities of Hoechst 33342 and SN-38 for ABCG2, suggesting a higher affinity of Hoechst 33342. The concentration-response curves are depicted in Figure 8 c.

Additionally, the antineoplastic drug mitoxantrone (MX) was used to demonstrate the reversal of resistance of the ABCG2 overexpressing MDCK II cells with compounds **14** and **47**. For this purpose, the cell viability was measured as described above after 72 h incubation with different modulator concentrations in the presence of 5 µM cytostatic. Decrease of cell viability caused by the cytotoxicity of the compound was taken into account by performing a dilution of the substance without MX. Wells with only cells and medium in presence and absence of MX were used as negative control. For both compounds, the reversal of resistance was demonstrated as shown in Figure 9. The half-maximal growth inhibition was achieved for compound **14** at 12.6 nM and for **47** at 22.0 nM, respectively. The same tendencies in reversing MDR as observed for SN-38 could be reproduced using MX as cytostatic as well as confirming the ability of the compounds to effectively reverse ABCG2 mediated MDR.

Investigation of ATPase Activity. ATPase measurements were carried out using High Five insect cell membranes, which were infected with baculovirus containing ABCG2 cDNA. Therefore, selected compounds based on scaffold A (4-substituted-2-phenylquinazolines) with high inhibitory potencies were investigated together with compounds comprising

scaffold B (4-methylpyrimidine). The determined EC_{50} values and the maximal stimulation caused by the compounds including quercetin as the standard activator are summarized in table 4. Three compounds (**13**, **14**, **17**) exhibited about the same activating effect as the standard quercetin. While most substances produced only low activation of less than 40%, having only a low effect on the ATPase activity. One compound (**48**) was inactive producing a stimulation of less than 10%. To confirm this unexpected result, the measurement was repeated six times. Compound **39** was the only compound in the data set exhibiting an inhibitory ATPase activity down to 40% of control. Interestingly there are two compounds, namely compound **26** and **27**, which demonstrate an increase of activation at lower concentrations on the one hand and a decrease of activation at higher concentrations on the other hand. About one-third of all investigated compounds showed an activation level between 140% to 160%.

Inspection of the EC_{50} values shows that in case of the methylpyrimidines with scaffold B a large difference in magnitude exists depending on the substituent at position two. Derivatives containing a pyridyl group (**42**, **43**, **44**) have EC_{50} values in the low nanomolar range, like the corresponding quinazolines with scaffold A (**17**, **21**, **22**). However, all investigated compounds with scaffold B and a 2-phenyl substituent (**45**, **46**, **47**) were much less potent with EC_{50} values in the micromolar range. The ATPase activation is only noticeable at concentrations far higher than the IC_{50} for ABCG2 inhibition. Therefore we investigated additionally some quinazolines from our previous publication containing a 2-phenyl substituent for their effect on ATPase activity (**49**, **51**, **53**). Interestingly for the quinazolines this difference between a 2-phenyl substituent and a pyridyl group in position 2, in activating efficacy is not apparent. Both groups of compounds are potent activators of ATPase activity with comparable EC_{50} values. But like most of the quinazolines (scaffold A) with a pyridyl substituent, the investigated 2-phenyl derivatives were found to exert only low stimulating effect of less than 50%.

While comparing the substitution pattern of scaffold A in relation to the position of the nitrogen atom in the pyridyl group, it becomes obvious that compounds comprising a 2-pyridyl moiety are less potent in ABCG2 inhibition assay as well as less effective in ATPase activation than their corresponding 3-pyridyl and 4-pyridyl analogs (**11**, **12**, **13** and **15**, **16**, **17**). Representative concentration-response curves of compounds **14**, **26, 39** and **quercetin** are illustrated in Figure 10. Compound **14**, being the most active with the lowest IC_{50} value in the Hoechst 33342 accumulation assay (64 nM), exhibited solely activation of ATPase activity over the whole range of concentrations similar to quercetin. Compound **26**, one of the two derivatives showing a bell-shaped curve, which is typical for substrates having different affinities for two distinct binding sites.[34, 35, 36] It is assumed that the transporter has two distinct binding sites for substrates, where the high affinity site is activating/transporting and the other one is inhibiting and has a low affinity for substrates. If both affinities are sufficiently different, a bell-shaped curve results. However, if the affinity to the activating binding site is several orders of magnitude higher than for the inhibitory site, a Michaelis-Menten type curve will be observed as only the activating site is targeted. The maximum of ATPase activity is reached at a concentration of about 0.5 μM with an activation of 55%. Further increase of concentration results in a decrease of ATPase activity going down to 25% at 35 μM. Fitting the data with a combination of an increasing and a decreasing logistic equation with a Hill coefficient fixed to one, an activating K_M of 9 nM and an inactivating K_i of 28000 nM was calculated. Although stimulation of ATPase activity is often considered as being typical for substrates, several direct and indirect evidence exists, that challenges this simple view. In the case of high ATPase activity stimulation, recently a fluorescent heterodimeric ABCG2 inhibitor comprised of a quinazoline and chalcone moiety was shown to accumulate in transfected MDCK II BCRP cells to the same extent as in parental cells not expressing ABCG2 using confocal fluorescence microscopy.[37] Further indirect evidence that the compounds are no substrates comes from the MTT data of their intrinsic cytotoxicity.

Here no differences between the GI_{50} values of the ABCG2 expressing and the parental cell line were observed, pointing to no or insufficient transport of the compounds. The same identical toxicity was observed in case of the quinazoline-chalcones. For further investigations of the binding mode of these compounds enzyme kinetic studies with the substrate Hoechst 33342 were undertaken.

Investigation of Inhibitory Enzyme Kinetics. Investigation of the mode of interaction was undertaken for compounds **14**, **21** and **26**, which were selected based on their different ATPase activity profiles. Studies were carried out with ABCG2 overexpressing MDCK II cells and Hoechst 33342. The Lineweaver-Burk linearization of the data for compound **14** proposes a non-competitive interaction with Hoechst 33342, as indicated by the intersection of the lines at the X-axis (Figure 11 a). Although linearization according to Lineweaver-Burk gives direct information on the type of interaction, this method has been criticized as being notoriously susceptible to experimental errors, due to the double reciprocal plot. Therefore we additionally analyzed the data using the method according to Hanes-Woolf. The half-reciprocal method according to Hanes-Woolf is claimed to be more robust to experimental errors. Compound **14** yielded an intersection of all lines at the X-axis, meaning that K_M remained constant but V_{max} decreased with increasing substrate concentrations that is characteristic for non-competitive inhibitors (Figure 11 d). Thus, both methods indicate a non-competitive interaction with Hoechst 33342 suggesting a different binding mode and/or binding pocket for compound **14**.

For compound **21,** on the other hand, a competitive interaction with Hoechst 33342 was derived from the Lineweaver-Burk linearization visualized by the intersection of the lines at the Y-axis (Figure 11 b). This result is substantiated by the results of the analysis according to Hanes-Woolf (Figure 11 e). Here an increase of K_M with higher inhibition concentrations is noticeable while V_{max} remains constant. According to both methods a competitive interaction

is proposed for compound **21**, suggesting the same binding mode and/or pocket as Hoechst 33342. Furthermore, the data of compound **26** were analyzed with the Lineweaver-Burk linearization obtaining straight lines with an intersection in the second quadrant of the coordinate system (Figure 11 c). This phenomenon is observed for "mixed-type" inhibitors with both, competitive and non-competitive characteristics. For instance, conformational change of the protein epitope upon binding of the "mixed-type" inhibitor can still affect the active site. Such inhibitors bind differently from the substrate but still influence substrate binding and turnover rate.

Applying the Hanes-Woolf method equivalent results were obtained, as indicated by decreasing V_{max} values und increasing K_M values with higher substrate concentrations in agreement with a non-competitive interaction of the "mixed type" (Figure 11 f).

As a third method the direct linear plot according to Cornish-Bowden was used to analyze the data. This method has been claimed to be insensitive to outliers. For compound **14** analysis of the data according to Cornish-Bowden reveals a decline of the maximal velocity V_{max} with increasing compound concentration while the Michaelis-Menten constant K_M remains the same, indicative of a non-competitive interaction with Hoechst 33342 (Figure 11 g). In compound **21** the plot of K_M (increasing) and V_{max} (constant) calculated from the analysis according to Cornish-Bowden (Fig. 11 h) nicely confirms previous results, exhibiting a competitive character. In Figure 11 i) a decreasing K_M and a slightly increasing V_{max} with increasing compound concentration is seen for compound **26** indicative of a mixed type of inhibition.

Conclusions

The purpose of this study was to extent the database of inhibitors based on a quinazoline scaffold. Notably, the comparison between 4-substituted 2-phenylquinazolines of our previous study and 4-substituted 2-pyridylquinazolines and 4-methylpyrimidine analogs with

lower molecular weight was targeted.[32] The investigation of the inhibitory activities against ABCG2 showed a distinct correlation between the position of the nitrogen atom in the pyridyl residue and the inhibitory potency: a nitrogen atom in *ortho* position resulted in less potent compounds while *meta* and *para* pyridyl substituents were found to be beneficial. Regarding the substitution at the aniline linker in position 4, nitro, cyano, trifluoromethyl and fluoro substituents yielded considerably high inhibitory activities toward ABCG2. The most potent compound in the test set contained a 3-pyridyl substitution at R^1 and a *para* nitro-group at R^2 (**14**) with an IC_{50} value of 64.1 nM, which is 3.5-fold lower than for compound **55**. Among the 4-methylpyrimidine derivatives based on scaffold B, several compounds yielded IC_{50} values between 100 and 150 nM. This demonstrates the extraordinary high ligand efficacy of this scaffold. For both scaffolds A and B, significant conformity regarding the IC_{50} value was observed between derivatives bearing pyridyl and phenyl, respectively. However, substitution with hydroxy on R^2 in *meta* and *para* was found to be significantly more favourable using a phenyl substitution at R^1. In general, the determined differences between the potencies of a *meta* or *para* substitution with the same residue is mentionable. Another advantage of the pyridyl derivatives compared to their phenyl analogs is the considerably lower calculated logP value that could be beneficial for bioavailability. For the whole test set however, no correlation between logP and pIC_{50} was found. Although sufficient lipophilicity is needed for membrane permeability, several compounds exhibit similar logP values but different inhibitory potencies. Hence, other determinants are probably influencing the potency of a compound to a higher degree. Furthermore, substitution with pyridyl yielded considerably lower cytotoxicities than with phenyl, resulting in several compounds with extraordinary high therapeutic ratios. Like for the IC_{50}, the GI_{50} of the compounds was often significantly influenced by the choice of substitution at R^2, as well as by the position in *meta* or *para*. Regarding selectivity toward ABCG2, only compounds with one or more methoxy groups showed activity toward ABCB1, while none of the selected compounds obtained a significant

activity toward ABCC1. The ability to reverse MDR was confirmed for the most potent compounds carrying out MDR reversal assays with the anticancer drugs SN-38 and MX. The IC_{50} values derived from the MTT assay often exceeded the inhibitory potency found in the Hoechst 33342 accumulation assays suggesting a higher affinity for Hoechst 33342 toward ABCG2.

Investigation of the effect on ATPase activity for selected compounds revealed four different types of ATPase activity curves. A small group of compounds showed solely an activating curve with high stimulating effect up to 85% in comparison to the basal activity. This group of compounds is comparable to quercetin, which is a well-known substrate of ABCG2 and shows high ATPase stimulating effects. Only one compound exhibited an inhibiting ATPase activity curve with 60% under the basal activity in the highest concentration. The third larger group of compounds comprises a half maximal ATPase activation of less than 50%. The last group illustrates a bell-shaped curve with a stimulation of ATPase activity by around 55% at the top of the curve and an inhibiting character at higher concentrations as also suggested in former studies[31, 32]. Interestingly, in the enzyme kinetic studies the same observations become obvious. Enzyme kinetic interaction studies with Hoechst 33342 as substrate with selected compounds exhibited three different modes of interaction: competitive, non-competitive and "mixed-type" inhibitors were identified using the double-reciprocal Lineweaver-Burk linearization, the half-reciprocal method according to Hanes-Woolf and the direct linear plot according to Cornish-Bowden. The results of all three methods were in accordance. The current study of 4-substituted 2-pyridylquinazolines showed to be a worthwhile continuation of the earlier studies of 4-substituted 2-phenylquinazolines: extended insights into the SAR of this new class of inhibitors regarding the inhibitory activity and selectivity toward ABCG2 together with the predominantly low cytotoxic effects observed in the MTT assay are some of the findings. Potential applicability for *in vivo* studies was confirmed by the high efficacy in reversing MDR when co-administered with the cytostatic agents SN-38 and MX. ATPase

results reflect the diversity of the compound interactions with the ABCG2 transport protein. This was also illustrated by the results of enzyme kinetic studies yielding different modes of interaction with the substrate Hoechst 33342.

Experimental Section

Chemistry. Materials. Chemicals were purchased from Acros Organics (Geel, Belgium), Alfa Aesar (Karlsruhe, Germany), Sigma Aldrich (Steinheim, Germany) or Merck (Darmstadt, Germany) and used without further purification. Microwave reactions were carried out in 50 ml vials with a CEM Discover SP (CEM GmbH, Kamp-Lintfort, Germany). Progress of the reaction was monitored by thin layer chromatography (TLC) using an aluminium plate coated with silica gel 60 F_{254} (Merck Millipore, Billerica, MA, USA). A mixture of dichloromethane and methanol (9:1) was used as eluent and the TLCs analyzed in a UV cabinet with an excitation wavelength of 254 nm. Identity of the compounds was confirmed by NMR. ^{1}H- and ^{13}C spectra were either obtained on a Bruker Advance 500 MHz (500/126 MHz) or Bruker Advance 600 MHz (600/151 MHz). DMSO-d6 was used as solvent for the compounds as well as internal standard to give chemical shifts (δ) expressed in ppm. Assignment of the ^{13}C signals was carried out by distortionless enhancement by polarization transfer (DEPT) and attached proton test (APT). The signals multiplicity is indicated as singulet (s), doublet (d), doublet of doublets (dd), triplet of doublets (td), triplet (t), doublet of triplets (dt), quartet (q) and multiplet (m). Coupling constants J are given in Hz. The purity of all biologically evaluated compounds was determined to be > 95% by elemental analysis recorded on a Vario EL V24 CHN Elemental Analyzer (Elementar Analysensysteme GmbH, Hanau, Germany). Found values were in the range of ± 0.4% of the theoretical values, unless indicated. Calculation of the logP values was performed with ACD/ChemSketch, file version C10E41, Advanced Chemistry Development, Inc., Toronto, ON, Canada, www.acdlabs.com, 2015.

General Procedure for the Preparation of the 2-Pyridylquinazolin-4(3*H*)-one Derivatives 1-3. A mixture of anthranilamide (2.72 g, 20 mmol), the corresponding pyridinecarboxaldehyde (20 mmol), iodine (3.17 g, 25 mmol), anhydrous potassium carbonate (2.76 g, 20 mmol) and 20 ml DMF was stirred at 70-90 °C for 4-8 h. The end of the reaction was monitored by TLC and the mixture poured on crushed ice to form a precipitate. Incomplete precipitation was prevented by adjusting the pH with concentrated HCl solution to about 7. After filtering off the precipitate, it was thoroughly washed with 100 mL of a 20% sodium thiosulfate solution followed by 100 mL of hot distilled water. Purification was performed by recrystallization from ethanol.

2-(Pyridin-2-yl)quinazolin-4(3H)-one (1). The compound was synthesized from picolinaldehyde (2.14 g, 20 mmol) as described in the general procedure for **1-3** to yield **1** as a white solid (3,84 g, 86%). ^{1}H NMR (500 MHz, DMSO-d_6) δ 11.77 (s, 1H), 8.76 (ddd, J = 4.7, 1.7, 0.9 Hz, 1H), 8.46 (dt, J = 7.9, 1.1 Hz, 1H), 8.18 (dd, J = 7.9, 1.5 Hz, 1H), 8.07 (td, J = 7.7, 1.7 Hz, 1H), 7.87 (ddd, J = 8.5, 7.0, 1.6 Hz, 1H), 7.80 (d, J = 8.0 Hz, 1H), 7.66 (ddd, J = 7.6, 4.8, 1.2 Hz, 1H), 7.57 (ddd, J = 8.1, 7.0, 1.2 Hz, 1H). ^{13}C NMR (126 MHz, DMSO) δ 149.1, 148.8, 138.1, 134.8, 127.8, 127.4, 126.7, 126.2, 122.3, 122.1.

2-(Pyridin-3-yl)quinazolin-4(3H)-one (2). The compound was synthesized from nicotinaldehyde (2.14 g, 20 mmol) as described in the general procedure for **1-3** to yield **2** as a white solid (3,34 g, 75%). ^{1}H NMR (500 MHz, DMSO-d_6) δ 12.70 (s, 1H), 9.30 (d, J = 2.3 Hz, 1H), 8.76 (dd, J = 4.8, 1.6 Hz, 1H), 8.51 (dt, J = 8.1, 1.9 Hz, 1H), 8.17 (dd, J = 7.9, 1.5 Hz, 1H), 7.85 (ddd, J = 8.5, 7.0, 1.6 Hz, 1H), 7.76 (dd, J = 8.2, 1.1 Hz, 1H), 7.60 (ddd, J = 8.0,

4.9, 0.8 Hz, 1H), 7.55 (ddd, *J* = 8.1, 7.1, 1.2 Hz, 1H). ^{13}C NMR (126 MHz, DMSO) δ 162.2, 151.7, 150.8, 148.7, 148.6, 135.8, 134.8, 129.0, 127.6, 127.1, 126.0, 123.7, 121.3.

2-(Pyridin-4-yl)quinazolin-4(3H)-one (3). The compound was synthesized from isonicotinaldehyde (2.14 g, 20 mmol) as described in the general procedure for **1-3** to yield **3** as a white solid (3,04 g, 68%). ^{1}H NMR (500 MHz, DMSO-d_6) δ 12.73 (s, 1H), 8.83 – 8.74 (m, 2H), 8.18 (dd, *J* = 7.9, 1.5 Hz, 1H), 8.14 – 8.08 (m, 2H), 7.87 (ddd, *J* = 8.5, 7.1, 1.6 Hz, 1H), 7.79 (dd, *J* = 8.2, 1.1 Hz, 1H), 7.58 (ddd, *J* = 8.1, 7.1, 1.2 Hz, 1H). ^{13}C NMR (126 MHz, DMSO) δ 162.1, 150.7, 150.3, 148.4, 140.1, 134.9, 127.9, 127.5, 126.1, 121.7, 121.6.

General Procedure for the Preparation of the 4-Chloro-2-pyridylquinazoline Derivatives 4-6.

The corresponding 2-pyridylquinazolin-4(3*H*)-one derivative (10 mmol) was added to phosphorus oxychloride (30 mL, 0.32 mol) and stirred for 10 min at room temperature. The mixture was then refluxed for 4-8 h and the reaction monitored by TLC. After completion of the reaction, excess $POCl_3$ was removed under reduced pressure and the residue poured in 50 mL ice water. Subsequently, 50 mL DCM was added while stirring and the pH of the mixture slowly adjusted to 7 with 25% ammonium solution. With a separatory funnel, the organic phase was collected, washed with 50 mL brine and dried over $MgSO_4$. The solvent was removed under reduced pressure and the obtained solid recrystallized from isopropanol.

4-Chloro-2-(pyridin-2-yl)quinazoline (4). The compound was synthesized from **1** (2.23 g, 10 mmol) as described in the general procedure for **4-6** to yield **4** as a white solid (2.15 g, 89%). ^{1}H NMR (500 MHz, DMSO-d_6) δ 8.77 (ddd, *J* = 4.8, 1.8, 1.0 Hz, 1H), 8.47 (dt, *J* = 7.9, 1.1 Hz, 1H), 8.21 – 8.14 (m, 1H), 8.09 (td, *J* = 7.8, 1.7 Hz, 1H), 7.87 (ddd, *J* = 8.5, 7.0, 1.6 Hz, 1H), 7.82 (dd, *J* = 7.9, 1.5 Hz, 1H), 7.67 (ddd, *J* = 7.6, 4.8, 1.2 Hz, 1H), 7.57 (ddd, *J* = 8.2, 7.0,

1.3 Hz, 1H). ^{13}C NMR (126 MHz, DMSO) δ 160.9, 150.1, 149.0, 148.4, 147.8, 138.1, 134.7, 127.3, 127.2, 126.7, 126.1, 122.3, 121.9.

4-Chloro-2-(pyridin-3-yl)quinazoline (5). The compound was synthesized from **2** (2.23 g, 10 mmol) as described in the general procedure for **4-6** to yield **5** as a white solid (2.27 g, 94%). ^{1}H NMR (500 MHz, DMSO-d_6) δ 9.29 (d, J = 2.2 Hz, 1H), 8.74 (dd, J = 4.8, 1.6 Hz, 1H), 8.49 (dt, J = 8.0, 2.0 Hz, 1H), 8.16 (dd, J = 7.9, 1.5 Hz, 1H), 7.84 (ddd, J = 8.5, 7.0, 1.6 Hz, 1H), 7.78 – 7.72 (m, 1H), 7.61 – 7.49 (m, 2H). ^{13}C NMR (126 MHz, DMSO) δ 162.2, 151.9, 150.9, 148.9, 148.6, 135.5, 134.8, 128.9, 127.7, 127.1, 126.0, 123.6, 121.3.

4-Chloro-2-(pyridin-4-yl)quinazoline (6). The compound was synthesized from **3** (2.23 g, 10 mmol) as described in the general procedure for **4-6** to yield **6** as a white solid (2.18 g, 90%). ^{1}H NMR (500 MHz, DMSO-d_6) δ 9.05 – 8.96 (m, 2H), 8.54 – 8.46 (m, 2H), 8.20 (dd, J = 8.0, 1.4 Hz, 1H), 7.90 (ddd, J = 8.5, 7.1, 1.6 Hz, 1H), 7.83 (dd, J = 8.3, 1.2 Hz, 1H), 7.62 (ddd, J = 8.1, 7.1, 1.2 Hz, 1H). ^{13}C NMR (126 MHz, DMSO) δ 162.0, 149.4, 148.0, 145.5, 145.0, 135.1, 128.2, 128.1, 126.1, 124.0, 121.8.

6-Methyl-2-(pyridin-4-yl)pyrimidin-4(3H)-one (7). To a solution of isonicotinimidamide hydrochloride (158 mg, 1 mmol) in methanol (5 mL) was added sodium methoxide (54.0 mg, 1 mmol) and stirred for 10 min at room temperature. After adding methyl acetoacetate (116 mg, 1 mmol) the mixture was transferred into a microwave tube, sealed and heated to 70 °C at 60 watt microwave irradiation for 4 h. After cooling to room temperature, the pH of the mixture was adjusted with 1 M hydrochloric acid to 7 and the formed precipitate filtered with suction. The solid was washed with water and dried in vacuo to give **7** as a white solid (76.8 mg, 41%). ^{1}H NMR (500 MHz, DMSO-d_6) δ 12.59 (s, 1H), 8.80 – 8.66 (m, 2H), 8.09 – 7.99 (m, 2H), 6.37 (s, 1H), 2.39 – 2.24 (m, 3H). ^{13}C NMR (126 MHz, DMSO) δ 150.4, 121.6, 23.5.

6-Methyl-2-phenylpyrimidin-4(3H)-one (8). This compound was sythesized according to the procedure described for **7**. Instead of isonicotinimidamide hydrochloride, benzimidamide hydrochloride (157 mg, 1 mmol) was used in the first step to yield **8** as a white solid (89.4 mg, 48%). ^{1}H NMR (500 MHz, DMSO-d_6) δ 12.47 (s, 1H), 8.22 – 7.99 (m, 2H), 7.60 – 7.42 (m, 3H), 6.19 (s, 1H), 2.26 (s, 3H). ^{13}C NMR (126 MHz, DMSO) δ 164.7, 163.9, 157.2, 132.9, 131.6, 128.7, 127.9, 110.0, 23.6.

General Procedure for the Preparation of the 2-Substituted 4-Chloro-6-methylpyrimidine Derivatives 9-10.

The compounds were synthesized according to the method described in the general methods for compounds **4-6** from the corresponding 2-substituted 6-methyl-pyrimidin-4(3H)-ones **7** and **8**. Complete chlorination was achieved within 4 h.

4-Chloro-6-methyl-2-(pyridin-4-yl)pyrimidine (9). The compound was synthesized from **7** (1.87 g, 10 mmol) as described in the general procedure for **9-10** to yield **9** as a white solid (1.79 g, 87%). ^{1}H NMR (600 MHz, DMSO-d_6) δ 8.81 – 8.74 (m, 2H), 8.21 – 8.16 (m, 2H), 7.69 (d, J = 0.7 Hz, 1H), 2.58 (s, 3H). ^{13}C NMR (151 MHz, DMSO) δ 170.6, 162.1, 160.9, 150.8, 143.0, 121.8, 120.8, 23.7.

4-Chloro-6-methyl-2-phenylpyrimidine (10). The compound was synthesized from **8** (1.86 g, 10 mmol) as described in the general procedure for **9-10** to yield **10** as a white solid (1.90 g, 93%). ^{1}H NMR (500 MHz, DMSO-d_6) δ 8.39 – 8.27 (m, 2H), 7.60 – 7.45 (m, 4H), 2.55 (d, J = 0.6 Hz, 3H). ^{13}C NMR (126 MHz, DMSO) δ 170.1, 163.8, 160.6, 135.9, 131.6, 128.9, 128.1, 119.0, 23.8.

General Procedure for the Preparation of the Substituted 4-Anilinoquinazolines 11-41.

The corresponding 4-chloroquinazoline derivative **4-6** (1 mmol) was added to isopropanol (5 mL) with the corresponding substituted aniline derivative (1 mmol) and sealed in a microwave tube. The mixture was heated by 100 watt microwave irradiation to 110 °C for a period of 15 – 30 min until completion of the reaction as indicated by TLC. The formed precipitate was filtered off, washed with 10 mL isopropanol and dried in vacuo. If no precipitate is formed, the solvent was removed under reduced pressure and the remaining solid recrystallized from ethanol.

N-(3-Nitrophenyl)-2-(pyridin-2-yl)quinazolin-4-amine (11).

The compound was synthesized from **4** (242 mg, 1 mmol) and 3-nitroaniline (138 mg, 1 mmol) as described in the general procedure for compounds **11-41** to yield **11** as a yellow solid (292 mg, 85%), mp 274-275 °C. ^{1}H NMR (500 MHz, DMSO-d_6) δ 12.09 (s, 1H), 9.09 (dd, J = 8.4, 1.3 Hz, 1H), 9.02 (t, J = 2.2 Hz, 1H), 8.93 (ddd, J = 4.8, 1.7, 0.9 Hz, 1H), 8.43 (dt, J = 7.9, 1.1 Hz, 1H), 8.39 (ddd, J = 8.1, 2.1, 0.9 Hz, 1H), 8.33 (dd, J = 8.5, 1.1 Hz, 1H), 8.24 – 8.17 (m, 2H), 8.14 (ddd, J = 8.5, 7.1, 1.2 Hz, 1H), 7.89 (ddd, J = 8.3, 7.1, 1.2 Hz, 1H), 7.86 – 7.78 (m, 2H). ^{13}C NMR (126 MHz, DMSO) δ 159.8, 154.9, 149.4, 148.3, 148.0, 141.4, 139.4, 138.5, 136.4, 130.2, 128.8, 128.2, 125.0, 124.7, 122.1, 120.6, 118.8, 113.8. Anal. Calcd. for $C_{19}H_{13}N_5O_2$: C, 66.47; H, 3.82; N, 20.40. Found: C, 66.38 ; H, 4.19; N, 20.16.

N-(3-Nitrophenyl)-2-(pyridin-3-yl)quinazolin-4-amine (12).

The compound was synthesized from **5** (242 mg, 1 mmol) and 3-nitroaniline (138 mg, 1 mmol) as described in the general procedure for compounds **11-41** to yield **12** as a yellow-beige solid (278 mg, 81%), mp >300 °C. ^{1}H NMR (500 MHz, DMSO-d_6) δ 10.51 (s, 1H), 9.61 (s, 1H), 9.17 (t, J = 2.2 Hz, 1H), 8.99 (dt, J = 8.1, 1.9 Hz, 1H), 8.84 (d, J = 4.9 Hz, 1H), 8.68 (dt, J = 8.4, 1.0 Hz, 1H), 8.36 (ddd, J = 8.2, 2.2, 0.9 Hz, 1H), 8.04 (ddd, J = 8.2, 2.3, 0.9

Hz, 1H), 8.01 – 7.95 (m, 2H), 7.81 (dd, *J* = 8.0, 5.0 Hz, 1H), 7.79 – 7.72 (m, 2H). ^{13}C NMR (126 MHz, DMSO) δ 158.2, 156.4, 149.9, 148.0, 140.4, 134.9, 134.3, 130.1, 128.2, 128.1, 127.3, 125.1, 123.5, 118.4, 116.5, 114.3. Anal. Calcd. for $C_{19}H_{13}N_5O_2$: C, 66.47; H, 3.82; N, 0.40. Found: C, 66.73; H, 4.10; N, 20.14.

N-(3-Nitrophenyl)-2-(pyridin-4-yl)quinazolin-4-amine (13).

The compound was synthesized from **6** (242 mg, 1 mmol) and 3-nitroaniline (138 mg, 1 mmol) as described in the general procedure for compounds **11-41** to yield **13** as a yellow solid (264 mg, 77%), mp >300 °C. ^{1}H NMR (500 MHz, DMSO-d_6) δ 10.59 (s, 1H), 9.16 (t, *J* = 2.2 Hz, 1H), 8.97 (d, *J* = 5.6 Hz, 2H), 8.73 (dt, *J* = 8.3, 1.0 Hz, 1H), 8.71 – 8.64 (m, 2H), 8.37 (ddd, *J* = 8.2, 2.2, 0.9 Hz, 1H), 8.07 – 7.97 (m, 3H), 7.83 – 7.73 (m, 2H). ^{13}C NMR (126 MHz, DMSO) δ 158.4, 155.5, 150.5, 150.0, 148.0, 145.5, 140.3, 134.4, 128.7, 128.2, 123.8, 123.6, 118.4, 116.6, 114.7. Anal. Calcd. for $C_{19}H_{13}N_5O_2$: C, 66.47; H, 3.82; N, 20.40. Found: C, 66.33; H, 4.20; N, 20.20.

N-(4-Nitrophenyl)-2-(pyridin-4-yl)quinazolin-4-amine (14).

The compound was synthesized from **5** (242 mg, 1 mmol) and 4-nitroaniline (138 mg, 1 mmol) as described in the general procedure for compounds **11-41** to yield **14** as a yellow solid (247 mg, 72%), mp >300 °C. ^{1}H NMR (500 MHz, DMSO-d_6) δ 10.72 (s, 1H), 9.64 – 9.55 (m, 1H), 9.13 (dt, *J* = 8.1, 1.8 Hz, 1H), 8.98 – 8.87 (m, 1H), 8.76 (dd, *J* = 8.3, 1.0 Hz, 1H), 8.39 – 8.33 (m, 2H), 8.33 – 8.27 (m, 2H), 8.04 – 7.94 (m, 3H), 7.76 (ddd, *J* = 8.3, 5.5, 2.7 Hz, 1H). ^{13}C NMR (126 MHz, DMSO) δ 158.2, 155.6, 149.8, 146.4, 145.6, 144.7, 142.6, 140.8, 135.2, 134.6, 128.0, 127.7, 126.2, 124.7, 123.8, 121.9, 114.6. Anal. Calcd. for $C_{19}H_{13}N_5O_2$: C, 66.47; H, 3.82; N, 20.40. Found: C, 66.52; H, 3.66; N, 20.15.

3-((2-(Pyridin-2-yl)quinazolin-4-yl)amino)benzonitrile (15).

The compound was synthesized from **4** (242 mg, 1 mmol) and 3-aminobenzonitrile (118 mg, 1 mmol) as described in the general procedure for compounds **11-41** to yield **15** as a light yellow solid (242 mg, 75%), mp 261-263 °C (decomp.). ^{1}H NMR (500 MHz, DMSO-d_6) δ 12.27 (s, 1H), 9.15 (dd, J = 8.3, 1.3 Hz, 1H), 8.92 (ddd, J = 4.8, 1.8, 0.9 Hz, 1H), 8.39 (t, J = 1.9 Hz, 1H), 8.33 (dd, J = 8.5, 1.1 Hz, 1H), 8.31 – 8.24 (m, 2H), 8.20 (td, J = 7.7, 1.7 Hz, 1H), 8.13 (ddd, J = 8.3, 7.0, 1.2 Hz, 1H), 7.87 (ddd, J = 8.3, 7.1, 1.2 Hz, 1H), 7.84 – 7.79 (m, 2H), 7.77 (t, J = 7.9 Hz, 1H). ^{13}C NMR (126 MHz, DMSO) δ 160.0, 154.9, 149.5, 148.2, 140.9, 139.3, 138.1, 136.5, 130.3, 129.9, 129.4, 128.8, 128.2, 127.9, 125.2, 124.5, 121.6, 118.5, 113.7, 111.7. Anal. Calcd. for $C_{20}H_{13}N_5$: C, 74.29; H, 4.05; N, 21.66. Found: C, 74.05; H, 4.34; N, 21.50.

3-((2-(Pyridin-3-yl)quinazolin-4-yl)amino)benzonitrile (16).

The compound was synthesized from **5** (242 mg, 1 mmol) and 3-aminobenzonitrile (118 mg, 1 mmol) as described in the general procedure for compounds **11-41** to yield **16** as a yellow solid (252 mg, 78%), mp >300 °C. ^{1}H NMR (500 MHz, DMSO-d_6) δ 10.17 (s, 1H), 9.52 (s, 1H), 8.68 (ddd, J = 9.9, 4.9, 3.0 Hz, 2H), 8.57 (dt, J = 8.4, 1.1 Hz, 1H), 8.45 (t, J = 1.8 Hz, 1H), 8.27 (ddd, J = 8.3, 2.2, 1.1 Hz, 1H), 7.96 – 7.90 (m, 2H), 7.73 – 7.65 (m, 2H), 7.62 (dt, J = 7.7, 1.3 Hz, 1H), 7.55 (ddd, J = 7.9, 4.7, 0.9 Hz, 1H). ^{13}C NMR (126 MHz, DMSO) δ 158.1, 157.5, 151.2, 150.5, 149.3, 140.2, 135.2, 133.9, 133.6, 130.1, 128.4, 127.3, 127.0, 126.8, 125.3, 123.8, 123.2, 118.9, 114.2, 111.5. Anal. Calcd. for $C_{20}H_{13}N_5$: C, 74.29; H, 4.05; N, 21.66. Found: C, 74.27; H, 4.22; N, 21.46.

3-((2-(Pyridin-4-yl)quinazolin-4-yl)amino)benzonitrile (17).

The compound was synthesized from **6** (242 mg, 1 mmol) and 3-aminobenzonitrile (118 mg, 1 mmol) as described in the general procedure for compounds **11-41** to yield **17** as a yellow solid (252 mg, 78%), mp >300 °C. ^{1}H NMR (500 MHz, DMSO-d_6) δ 10.62 (s, 1H), 9.04 – 8.94 (m, 2H), 8.81 – 8.72 (m, 1H), 8.68 – 8.60 (m, 2H), 8.36 (t, J = 1.8 Hz, 1H), 8.31 (dt, J =

7.8, 1.9 Hz, 1H), 8.03 – 7.95 (m, 2H), 7.77 (ddd, *J* = 8.3, 5.7, 2.5 Hz, 1H), 7.71 – 7.63 (m, 2H). ^{13}C NMR (126 MHz, DMSO) δ 158.5, 155.1, 151.5, 149.8, 144.3, 139.8, 134.4, 130.1, 128.5, 128.2, 127.7, 127.5, 125.8, 124.2, 123.8, 118.8, 114.7, 111.6. Anal. Calcd. for $C_{20}H_{13}N_5$: C, 74.29; H, 4.05; N, 21.66. Found: C, 74.66; H, 4.32; N, 21.40.

4-((2-(Pyridin-3-yl)quinazolin-4-yl)amino)benzonitrile (18).

The compound was synthesized from **5** (242 mg, 1 mmol) and 4-aminobenzonitrile (118 mg, 1 mmol) as described in the general procedure for compounds **11-41** to yield **18** as a light yellow solid (278 mg, 86%), mp 285-287 °C (decomp.). ^{1}H NMR (500 MHz, DMSO-d_6) δ 10.75 (s, 1H), 9.54 (d, *J* = 2.0 Hz, 1H), 9.12 (dt, *J* = 8.1, 1.8 Hz, 1H), 8.95 (dd, *J* = 5.4, 1.5 Hz, 1H), 8.83 – 8.74 (m, 1H), 8.24 – 8.16 (m, 2H), 8.05 – 7.94 (m, 3H), 7.93 – 7.85 (m, 2H), 7.73 (ddd, *J* = 8.3, 6.6, 1.6 Hz, 1H). ^{13}C NMR (126 MHz, DMSO) δ 158.3, 155.2, 149.1, 145.8, 144.0, 143.3, 141.4, 135.1, 134.6, 133.0, 127.7, 127.5, 126.4, 124.0, 122.7, 119.2, 114.5, 105.79. Anal. Calcd. for $C_{20}H_{13}N_5$: C, 74.29; H, 4.05; N, 21.66. Found: C, 74.42; H, 4.33; N, 21.33.

N-(3-Methoxyphenyl)-2-(pyridin-2-yl)quinazolin-4-amine (19).

The compound was synthesized from **4** (242 mg, 1 mmol) and 3-methoxyaniline (123 mg, 1 mmol) as described in the general procedure for compounds **11-41** to yield **19** as a yellow solid (207 mg, 63%), mp 115-117 °C. ^{1}H NMR (500 MHz, DMSO-d_6) δ 9.83 (s, 1H), 8.78 – 8.68 (m, 1H), 8.64 (d, *J* = 8.2 Hz, 1H), 8.44 (dt, *J* = 8.0, 1.1 Hz, 1H), 8.27 (t, *J* = 2.2 Hz, 1H), 8.00 – 7.86 (m, 3H), 7.66 (ddd, *J* = 8.3, 6.6, 1.5 Hz, 1H), 7.56 (ddd, *J* = 8.2, 2.0, 0.9 Hz, 1H), 7.50 (ddd, *J* = 7.6, 4.7, 1.2 Hz, 1H), 7.30 (t, *J* = 8.1 Hz, 1H), 6.69 (ddd, *J* = 8.2, 2.5, 0.9 Hz, 1H), 3.88 (s, 3H). ^{13}C NMR (126 MHz, DMSO) δ 159.6, 159.0, 158.1, 155.8, 150.6, 149.6, 141.1, 136.9, 133.4, 129.2, 128.6, 126.7, 124.8, 123.5, 123.1, 114.5, 113.7, 109.9, 107.0, 55.3. Anal. Calcd. for $C_{20}H_{16}N_4O$; C, 73.15; H, 4.91; N, 17.06. Found: C, 73.43; H, 5.27; N, 16.99.

N-(3-Methoxyphenyl)-2-(pyridin-3-yl)quinazolin-4-amine (20).

The compound was synthesized from **5** (242 mg, 1 mmol) and 3-methoxyaniline (123 mg, 1 mmol) as described in the general procedure for compounds **11-41** to yield **20** as a light yellow solid (213 mg, 65%), mp 182-184 °C. ^{1}H NMR (500 MHz, DMSO-d_6) δ 9.88 (s, 1H), 9.56 (d, J = 2.0 Hz, 1H), 8.72 – 8.65 (m, 2H), 8.60 (dt, J = 8.4, 1.1 Hz, 1H), 7.92 – 7.85 (m, 2H), 7.70 (t, J = 2.3 Hz, 1H), 7.67 – 7.61 (m, 1H), 7.58 – 7.50 (m, 2H), 7.36 (t, J = 8.1 Hz, 1H), 6.76 (ddd, J = 8.2, 2.6, 0.8 Hz, 1H), 3.82 (s, 3H). ^{13}C NMR (126 MHz, DMSO) δ 159.6, 158.1, 157.6, 151.1, 150.4, 149.3, 140.5, 135.2, 133.8, 133.6, 129.4, 128.3, 126.5, 123.7, 123.2, 114.6, 114.3, 109.8, 107.9, 55.3. Anal. Calcd. for $C_{20}H_{16}N_4O$; C, 73.15; H, 4.91; N, 17.06. Found: C, 73.20; H, 4.82; N, 17.11.

N-(3-Methoxyphenyl)-2-(pyridin-4-yl)quinazolin-4-amine (21).

The compound was synthesized from **6** (242 mg, 1 mmol) and 3-methoxyaniline (123 mg, 1 mmol) as described in the general procedure for compounds **11-41** to yield **21** as a light beige solid (230 mg, 70%), mp 202-203 °C. ^{1}H NMR (500 MHz, DMSO-d_6) δ 9.92 (s, 1H), 8.79 – 8.69 (m, 2H), 8.61 (dt, J = 8.4, 1.0 Hz, 1H), 8.32 – 8.24 (m, 2H), 7.97 – 7.86 (m, 2H), 7.72 – 7.64 (m, 2H), 7.56 (ddd, J = 8.0, 2.0, 0.9 Hz, 1H), 7.37 (t, J = 8.1 Hz, 1H), 6.76 (ddd, J = 8.2, 2.5, 0.9 Hz, 1H), 3.83 (s, 3H). ^{13}C NMR (126 MHz, DMSO) δ 159.6, 158.3, 157.4, 150.4, 150.3, 145.7, 140.4, 133.6, 129.4, 128.5, 127.0, 123.3, 121.9, 114.6, 109.9, 107.8, 55.3. Anal. Calcd. for $C_{20}H_{16}N_4O$; C, 73.15; H, 4.91; N, 17.06. Found: C, 73.42; H, 4.69; N,17.00.

N-(4-Methoxyphenyl)-2-(pyridin-4-yl)quinazolin-4-amine (22).

The compound was synthesized from **6** (242 mg, 1 mmol) and 4-methoxyaniline (123 mg, 1 mmol) as described in the general procedure for compounds **11-41** to yield **22** as a light yellow solid (233 mg, 71%), mp 233-235 °C (decomp.). ^{1}H NMR (500 MHz, DMSO-d_6) δ

9.89 (s, 1H), 8.76 – 8.68 (m, 2H), 8.56 (dt, *J* = 8.2, 1.0 Hz, 1H), 8.28 – 8.20 (m, 2H), 7.93 – 7.85 (m, 2H), 7.85 – 7.76 (m, 2H), 7.65 (ddd, *J* = 8.3, 4.7, 3.4 Hz, 1H), 7.09 – 7.00 (m, 2H), 3.81 (s, 3H). ^{13}C NMR (126 MHz, DMSO) δ 158.4, 157.5, 156.1, 150.3, 150.2, 145.8, 133.4, 132.0, 128.4, 126.8, 124.4, 123.2, 121.9, 114.5, 113.9, 55.4. Anal. Calcd. for $C_{20}H_{16}N_4O$; C, 73.15; H, 4.91; N, 17.06. Found: C, 73.43; H, 5.01; N, 16.75.

N-(3,4-Dimethoxyphenyl)-2-(pyridin-2-yl)quinazolin-4-amine (23).

The compound was synthesized from **4** (242 mg, 1 mmol) and 3,4-dimethoxyaniline (153 mg, 1 mmol) as described in the general procedure for compounds **11-41** to yield **23** as a yellow solid (204 mg, 57%), mp 191-193 °C. ^{1}H NMR (500 MHz, DMSO-d_6) δ 9.82 (s, 1H), 8.72 (ddd, *J* = 4.7, 1.9, 0.9 Hz, 1H), 8.65 – 8.57 (m, 1H), 8.45 (dt, *J* = 7.9, 1.1 Hz, 1H), 8.37 (d, *J* = 2.5 Hz, 1H), 7.96 (td, *J* = 7.7, 1.8 Hz, 1H), 7.94 – 7.85 (m, 2H), 7.65 (ddd, *J* = 8.3, 6.6, 1.6 Hz, 1H), 7.50 (ddd, *J* = 7.5, 4.7, 1.2 Hz, 1H), 7.43 (dd, *J* = 8.7, 2.5 Hz, 1H), 7.00 (d, *J* = 8.7 Hz, 1H), 3.91 (s, 3H), 3.78 (s, 3H). ^{13}C NMR (126 MHz, DMSO) δ 159.0, 157.9, 155.7, 149.5, 148.5, 145.1, 136.9, 133.3, 128.3, 126.6, 124.8, 123.5, 123.0, 114.3, 113.3, 112.0, 107.2, 55.9, 55.6. Anal. Calcd. for $C_{21}H_{18}N_4O_2$; C, 70.38; H, 5.06; N, 15.63. Found: C, 70.01; H, 5.31; N, 15.95.

N-(3,4-Dimethoxyphenyl)-2-(pyridin-3-yl)quinazolin-4-amine (24).

The compound was synthesized from **5** (242 mg, 1 mmol) and 3,4-dimethoxyaniline (153 mg, 1 mmol) as described in the general procedure for compounds **11-41** to yield **24** as a yellow solid (240 mg, 67%), mp 201-202 °C. ^{1}H NMR (500 MHz, DMSO-d_6) δ 10.76 (s, 1H), 9.51 (d, *J* = 2.2 Hz, 1H), 8.97 (dt, *J* = 8.1, 1.8 Hz, 1H), 8.89 (dd, *J* = 5.1, 1.6 Hz, 1H), 8.77 (d, *J* = 8.2 Hz, 1H), 8.11 (d, *J* = 8.3 Hz, 1H), 7.99 (ddd, *J* = 8.4, 7.0, 1.3 Hz, 1H), 7.87 (dd, *J* = 8.1, 5.1 Hz, 1H), 7.75 (ddd, *J* = 8.3, 7.0, 1.2 Hz, 1H), 7.59 (d, *J* = 2.4 Hz, 1H), 7.40 (dd, *J* = 8.6, 2.5 Hz, 1H), 7.07 (d, *J* = 8.7 Hz, 1H), 3.81 (s, 3H), 3.81 (s, 3H). ^{13}C NMR (126 MHz, DMSO) δ

158.5, 155.7, 148.6, 146.7, 134.8, 131.1, 127.7, 125.2, 124.0, 115.8, 113.8, 111.8, 108.6, 55.9, 55.8. Anal. Calcd. for $C_{21}H_{18}N_4O_2$; C, 70.38; H, 5.06; N, 15.63. Found: C, 70.41; H, 4.93; N, 15.34.

N-(3,4-Dimethoxyphenyl)-2-(pyridin-4-yl)quinazolin-4-amine (25).

The compound was synthesized from **6** (242 mg, 1 mmol) and 3,4-dimethoxyaniline (153 mg, 1 mmol) as described in the general procedure for compounds **11-41** to yield **25** as a yellow solid (219 mg, 61%), mp 134-135 °C. ^{1}H NMR (500 MHz, DMSO-d_6) δ 9.86 (s, 1H), 8.78 – 8.69 (m, 2H), 8.58 (dt, J = 8.5, 1.0 Hz, 1H), 8.31 – 8.24 (m, 2H), 7.93 – 7.86 (m, 2H), 7.72 – 7.61 (m, 2H), 7.46 (dd, J = 8.6, 2.5 Hz, 1H), 7.06 (d, J = 8.7 Hz, 1H), 3.83 (s, 3H), 3.80 (s, 3H). ^{13}C NMR (126 MHz, DMSO) δ 158.2, 157.5, 150.3, 148.5, 145.8, 133.5, 132.5, 128.4, 126.9, 123.1, 121.9, 114.6, 112.0, 107.8, 55.9, 55.7. Anal. Calcd. for $C_{21}H_{18}N_4O_2$; C, 70.38; H, 5.06; N, 15.63. Found: C, 70.70; H, 5.05; N, 15.28.

2-(Pyridin-4-yl)-N-(3-(trifluoromethyl)phenyl)quinazolin-4-amine (26).

The compound was synthesized from **6** (242 mg, 1 mmol) and 3-(trifluoromethyl)aniline (161 mg, 1 mmol) as described in the general procedure for compounds **11-41** to yield **26** as a white solid (322 mg, 88%), mp 249-250 °C (decomp.). ^{1}H NMR (500 MHz, DMSO-d_6) δ 10.21 (s, 1H), 8.74 (d, J = 5.0 Hz, 2H), 8.62 (dt, J = 8.3, 1.0 Hz, 1H), 8.57 (d, J = 2.0 Hz, 1H), 8.32 – 8.24 (m, 2H), 8.21 (dd, J = 8.3, 2.0 Hz, 1H), 7.99 – 7.88 (m, 2H), 7.76 – 7.65 (m, 2H), 7.52 (ddd, J = 7.8, 1.9, 0.9 Hz, 1H). ^{13}C NMR (126 MHz, DMSO) δ 158.2, 157.2, 150.4, 150.3, 145.5, 140.1, 133.9, 129.9, 129.4 (d, J = 31.6 Hz), 128.6, 127.3, 125.7, 123.2, 121.8, 120.0 (d, J = 3.9 Hz), 118.5 (d, J = 4.1 Hz), 114.5. Anal. Calcd. for $C_{20}H_{13}F_3N_4$; C, 65.57; H, 3.58; N, 15.29. Found: C, 65.53; H, 3.93; N, 14.90.

2-(Pyridin-4-yl)-N-(4-(trifluoromethyl)phenyl)quinazolin-4-amine (27).

The compound was synthesized from **6** (242 mg, 1 mmol) and 4-(trifluoromethyl)aniline (161 mg, 1 mmol) as described in the general procedure for compounds **11-41** to yield **27** as a white solid (308 mg, 84%), mp 264-265 °C (decomp.). ^{1}H NMR (500 MHz, DMSO-d_6) δ 10.22 (s, 1H), 8.83 – 8.68 (m, 2H), 8.64 (dt, J = 8.4, 1.1 Hz, 1H), 8.34 – 8.27 (m, 2H), 8.28 – 8.19 (m, 2H), 7.98 – 7.91 (m, 2H), 7.87 – 7.80 (m, 2H), 7.72 (ddd, J = 8.3, 5.4, 2.8 Hz, 1H). ^{13}C NMR (126 MHz, DMSO) δ 158.2, 157.2, 150.4, 150.4, 145.5, 143.0, 134.0, 128.6, 127.29, 125.9 (d, J = 3.6 Hz), 123.6 (d, J = 32.1 Hz), 123.4, 122.0, 121.9, 114.6. Anal. Calcd. for $C_{20}H_{13}F_3N_4$; C, 65.57; H, 3.58; N, 15.29. Found: C, 65.29; H, 3.86; N, 15.20.

N-(4-Methoxy-3-(trifluoromethyl)phenyl)-2-(pyridin-4-yl)quinazolin-4-amine (28).

The compound was synthesized from **6** (242 mg, 1 mmol) and 4-methoxy-3-(trifluoromethyl)aniline (191 mg, 1 mmol) as described in the general procedure for compounds **11-41** to yield **28** as a light beige solid (226 mg, 57%), mp 256-257 °C (decomp.). ^{1}H NMR (500 MHz, DMSO-d_6) δ 10.06 (s, 1H), 8.76 – 8.68 (m, 2H), 8.57 (dt, J = 8.4, 1.1 Hz, 1H), 8.39 (d, J = 2.7 Hz, 1H), 8.28 – 8.22 (m, 2H), 8.17 (dd, J = 9.0, 2.7 Hz, 1H), 7.95 – 7.88 (m, 2H), 7.69 (ddd, J = 8.3, 5.0, 3.2 Hz, 1H), 7.40 (d, J = 9.1 Hz, 1H), 3.94 (s, 3H). ^{13}C NMR (126 MHz, DMSO) δ 158.2, 157.3, 153.3, 150.3, 150.2, 145.6, 133.7, 132.0, 128.5, 127.7, 127.1, 125.0, 123.1, 122.8, 121.8, 120.9 (d, J = 5.8 Hz), 116.6 (d, J = 30.2 Hz), 114.5, 113.4, 56.5. Anal. Calcd. for $C_{21}H_{15}F_3N_4O$; C, 63.63; H, 3.81; N, 14.14. Found: C, 63.87; H, 3.87; N, 13.76.

N-(3-Fluorophenyl)-2-(pyridin-3-yl)quinazolin-4-amine (29).

The compound was synthesized from **5** (242 mg, 1 mmol) and 3-fluoroaniline (111 mg, 1 mmol) as described in the general procedure for compounds **11-41** to yield **29** as a yellow solid (253 mg, 80%), mp 272-274 °C (decomp.) . ^{1}H NMR (500 MHz, DMSO-d_6) δ 10.60 (s,

1H), 9.52 (d, *J* = 2.0 Hz, 1H), 9.04 (dt, *J* = 8.1, 1.9 Hz, 1H), 8.91 (dd, *J* = 5.3, 1.5 Hz, 1H), 8.76 (d, *J* = 8.2 Hz, 1H), 8.10 – 8.01 (m, 1H), 8.01 – 7.98 (m, 1H), 7.98 – 7.92 (m, 1H), 7.89 (dt, *J* = 11.6, 2.4 Hz, 1H), 7.82 – 7.76 (m, 1H), 7.74 (ddd, *J* = 8.1, 6.6, 1.3 Hz, 1H), 7.51 (td, *J* = 8.2, 6.8 Hz, 1H), 7.06 (td, *J* = 8.5, 2.6 Hz, 1H). ^{13}C NMR (126 MHz, DMSO) δ 163.1, 161.2, 158.5, 155.7, 145.2, 140.4 (d, *J* = 10.9 Hz), 134.5, 130.3 (d, *J* = 9.4 Hz), 127.6, 126.8, 125.8, 123.8, 118.8, 111.2 (d, *J* = 21.2 Hz), 109.8 (d, *J* = 25.7 Hz). Anal. Calcd. for $C_{19}H_{13}FN_4$; C, 72.14; H, 4.14; N, 17.71. Found: C, 72.13; H, 4.38; N, 17.69.

3-((2-(Pyridin-4-yl)quinazolin-4-yl)amino)benzenesulfonyl fluoride (30).

The compound was synthesized from **6** (242 mg, 1 mmol) and 3-aminobenzenesulfonyl fluoride (175 mg, 1 mmol) as described in the general procedure for compounds **11-41** to yield **30** as a yellow solid (293 mg, 77%), mp 291-292 °C (decomp.). ^{1}H NMR (600 MHz, DMSO-d_6) δ 10.40 (s, 1H), 9.14 (t, *J* = 1.9 Hz, 1H), 8.73 (d, *J* = 5.1 Hz, 2H), 8.62 (d, *J* = 8.4 Hz, 1H), 8.42 (dt, *J* = 7.2, 2.1 Hz, 1H), 8.35 – 8.26 (m, 2H), 8.01 – 7.92 (m, 2H), 7.92 – 7.83 (m, 2H), 7.74 (ddd, *J* = 8.2, 5.5, 2.7 Hz, 1H). ^{13}C NMR (151 MHz, DMSO) δ 158.1, 157.1, 150.4, 150.4, 145.2, 141.0, 134.1, 131.9 (d, *J* = 23.1 Hz), 131.0, 129.0, 128.7, 127.5, 123.3, 122.8, 121.9, 120.6, 114.5. Anal. Calcd. for $C_{19}H_{13}FN_4O_2S$; C, 59.99; H, 3.44; N, 14.73. Found: C, 60.36; H, 3.68; N, 14.48.

N1,N1-Dimethyl-N3-(2-(pyridin-3-yl)quinazolin-4-yl)benzene-1,3-diamine (31).

The compound was synthesized from **5** (242 mg, 1 mmol) and N1,N1-dimethylbenzene-1,3-diamine (136 mg, 1 mmol) as described in the general procedure for compounds **11-41** to yield **31** as a light brown solid (201 mg, 59%), mp 202-203 °C.^{1}H NMR (500 MHz, DMSO-d_6) δ 10.87 (s, 1H), 9.62 – 9.48 (m, 1H), 9.18 (d, *J* = 8.1 Hz, 1H), 9.02 – 8.90 (m, 1H), 8.83 (dd, *J* = 8.5, 1.4 Hz, 1H), 8.11 (d, *J* = 8.3 Hz, 1H), 8.01 (ddd, *J* = 8.4, 5.9, 1.3 Hz, 3H), 7.76 (ddd, *J* = 8.3, 7.0, 1.2 Hz, 1H), 7.62 (s, 1H), 7.51 (t, *J* = 8.1 Hz, 1H), 7.25 (s, 1H), 3.09 (s, 6H).

^{13}C NMR (126 MHz, DMSO) δ 158.6, 155.2, 141.3, 139.3, 134.8, 129.9, 127.9, 126.1, 124.1, 114.1, 43.5. Anal. Calcd. for $C_{21}H_{19}N_5$; C, 73.88; H, 5.61; N, 20.51. Found: C, 73.97; H, 5.37; N, 20.25.

3-((2-(Pyridin-4-yl)quinazolin-4-yl)amino)phenol (32).

The compound was synthesized from **6** (242 mg, 1 mmol) and 3-aminophenol (109 mg, 1 mmol) as described in the general procedure for compounds **11-41** to yield **32** as a yellow solid (148 mg, 47%), mp > 300 °C. ^{1}H NMR (500 MHz, DMSO-d_6) δ 10.13 (s, 1H), 9.60 (s, 1H), 8.97 – 8.91 (m, 2H), 8.70 (dt, J = 8.4, 0.9 Hz, 1H), 8.65 – 8.58 (m, 2H), 8.01 – 7.90 (m, 2H), 7.73 (ddd, J = 8.3, 6.5, 1.7 Hz, 1H), 7.44 (t, J = 2.2 Hz, 1H), 7.36 (ddd, J = 8.0, 2.0, 1.0 Hz, 1H), 7.25 (t, J = 8.0 Hz, 1H), 6.64 (ddd, J = 8.1, 2.4, 1.0 Hz, 1H). ^{13}C NMR (126 MHz, DMSO) δ 158.5, 157.7, 155.8, 149.3, 145.7, 139.7, 134.1, 129.3, 128.1, 127.8, 123.8, 123.6, 114.7, 113.6, 111.8, 110.0. Anal. Calcd. for $C_{19}H_{14}N_4O$; C, 72.60; H, 4.49; N, 17.82. Found: C, 72.86; H, 4.63; N, 17.44.

4-((2-(Pyridin-4-yl)quinazolin-4-yl)amino)phenol (33).

The compound was synthesized from **6** (242 mg, 1 mmol) and 4-aminophenol (109 mg, 1 mmol) as described in the general procedure for compounds **11-41** to yield **33** as a yellow solid (182 mg, 58%), mp 293-295 °C (decomp).^{1}H NMR (500 MHz, DMSO-d_6) δ 10.34 (s, 1H), 9.52 (s, 1H), 8.96 (d, J = 5.7 Hz, 2H), 8.73 – 8.63 (m, 1H), 8.63 – 8.50 (m, 2H), 8.00 (dd, J = 8.4, 1.3 Hz, 1H), 7.95 (ddd, J = 8.2, 6.8, 1.2 Hz, 1H), 7.72 (ddd, J = 8.2, 6.9, 1.4 Hz, 1H), 7.67 – 7.56 (m, 2H), 6.94 – 6.84 (m, 2H). ^{13}C NMR (126 MHz, DMSO) δ 158.7, 155.4, 155.0, 134.2, 129.6, 127.9, 125.2, 123.9, 123.6, 115.3, 114.4. Anal. Calcd. for $C_{19}H_{14}N_4O$; C, 72.60; H, 4.49; N, 17.82. Found: C, 72.69; H, 4.67; N, 17.54.

(4-((2-(Pyridin-3-yl)quinazolin-4-yl)amino)phenyl)methanol (34).

The compound was synthesized from **5** (242 mg, 1 mmol) and (3-aminophenyl)methanol (123 mg, 1 mmol) as described in the general procedure for compounds **11-41** to yield **34** as a yellow solid (210 mg, 64%), mp > 300 °C.^{1}H NMR (500 MHz, DMSO-d_6) δ 10.65 (s, 1H), 9.56 (d, J = 2.1 Hz, 1H), 9.07 (dt, J = 8.1, 1.9 Hz, 1H), 8.92 (dd, J = 5.2, 1.6 Hz, 1H), 8.83 – 8.73 (m, 1H), 8.08 (d, J = 8.3 Hz, 1H), 8.05 – 7.97 (m, 2H), 7.91 (dd, J = 8.1, 5.2 Hz, 1H), 7.82 – 7.73 (m, 2H), 7.45 (t, J = 7.8 Hz, 1H), 7.20 (d, J = 7.5 Hz, 1H), 4.63 (s, 2H). ^{13}C NMR (126 MHz, DMSO) δ 158.6, 155.7, 143.3, 138.2, 134.6, 128.4, 127.6, 125.5, 123.9, 123.0, 121.6, 121.4, 114.1, 62.9. Anal. Calcd. for $C_{20}H_{16}N_4O$; C, 73.15; H, 4.91; N, 17.06. Found: C, 73.17; H, 5.07; N, 16.83.

(4-((2-(Pyridin-4-yl)quinazolin-4-yl)amino)phenyl)methanol (35).

The compound was synthesized from **6** (242 mg, 1 mmol) and (3-aminophenyl)methanol (123 mg, 1 mmol) as described in the general procedure for compounds **11-41** to yield **35** as a yellow solid (200 mg, 61%), mp > 300 °C. ^{1}H NMR (500 MHz, DMSO-d_6) δ 10.36 (s, 1H), 8.97 (d, J = 5.7 Hz, 2H), 8.80 – 8.60 (m, 3H), 8.06 (t, J = 1.9 Hz, 1H), 8.03 – 7.90 (m, 2H), 7.81 – 7.68 (m, 2H), 7.42 (t, J = 7.8 Hz, 1H), 7.19 – 7.12 (m, 1H), 4.62 (s, 2H). ^{13}C NMR (126 MHz, DMSO) δ 158.5, 155.3, 149.2, 144.5, 143.3, 138.6, 134.2, 128.3, 128.0, 124.2, 123.7, 122.5, 121.1, 121.0, 114.6, 62.9. Anal. Calcd. for $C_{20}H_{16}N_4O$; C, 73.15; H, 4.91; N, 17.06. Found: C, 73.06; H, 5.27; N, 16.69.

2-Nitro-4-((2-(pyridin-3-yl)quinazolin-4-yl)amino)phenol (36).

The compound was synthesized from **5** (242 mg, 1 mmol) and 4-amino-2-nitrophenol (154 mg, 1 mmol) as described in the general procedure for compounds **11-41** to yield **36** as a yellow-orange solid (223 mg, 62%), mp 284-286 °C (decomp.).^{1}H NMR (500 MHz, DMSO-

d_6) δ 10.83 (s, 1H), 10.06 (s, 1H), 9.56 (dd, J = 2.2, 0.9 Hz, 1H), 8.78 (d, J = 2.7 Hz, 1H), 8.74 – 8.70 (m, 1H), 8.68 (dd, J = 4.7, 1.7 Hz, 1H), 8.54 (dt, J = 8.4, 1.1 Hz, 1H), 8.04 (dd, J = 9.0, 2.7 Hz, 1H), 7.92 – 7.86 (m, 2H), 7.68 – 7.61 (m, 1H), 7.56 – 7.50 (m, 1H), 7.24 (d, J = 9.0 Hz, 1H). ^{13}C NMR (126 MHz, DMSO) δ 158.0, 157.5, 151.1, 150.3, 149.4, 149.0, 135.7, 135.3, 133.7, 133.6, 131.0, 130.3, 128.4, 126.6, 123.7, 123.1, 119.4, 118.4, 114.2. Anal. Calcd. for $C_{19}H_{13}N_5O_3$; C, 63.51; H, 3.65; N, 19.49. Found: C, 63.90; H, 3.81; N, 19.21.

Methyl 3-((2-(pyridin-3-yl)quinazolin-4-yl)amino)benzoate (37).

The compound was synthesized from **5** (242 mg, 1 mmol) and methyl 3-aminobenzoate (151 mg, 1 mmol) as described in the general procedure for compounds **11-41** to yield **37** as a light yellow solid (282 mg, 79%), mp 233-234 °C.^{1}H NMR (600 MHz, DMSO-d_6) δ 10.73 (s, 1H), 9.55 (d, J = 2.1 Hz, 1H), 9.09 (dt, J = 8.2, 1.8 Hz, 1H), 8.92 (dd, J = 5.4, 1.5 Hz, 1H), 8.84 – 8.70 (m, 2H), 8.20 (ddd, J = 8.1, 2.3, 1.1 Hz, 1H), 8.08 – 8.01 (m, 1H), 8.01 – 7.90 (m, 2H), 7.80 (dt, J = 7.8, 1.3 Hz, 1H), 7.74 (ddd, J = 8.3, 6.9, 1.3 Hz, 1H), 7.62 (t, J = 7.9 Hz, 1H), 3.92 (s, 3H). ^{13}C NMR (151 MHz, DMSO) δ 166.3, 158.5, 155.5, 145.1, 140.3, 139.0, 134.6, 130.2, 129.2, 127.7, 127.3, 126.5, 125.9, 125.2, 123.9, 123.4, 114.2, 52.6. Anal. Calcd. for $C_{21}H_{16}N_4O_2$; C, 70.77; H, 4.53; N, 15.72. Found: C, 71.08; H, 4.62; N, 15.49.

Methyl 3-((2-(pyridin-4-yl)quinazolin-4-yl)amino)benzoate (38).

The compound was synthesized from **6** (242 mg, 1 mmol) and methyl 3-aminobenzoate (151 mg, 1 mmol) as described in the general procedure for compounds **11-41** to yield **38** as a yellow solid (256 mg, 76%), mp 251-252 °C (decomp.). ^{1}H NMR (600 MHz, DMSO-d_6) δ 10.46 (s, 1H), 9.01 – 8.94 (m, 2H), 8.81 (t, J = 2.0 Hz, 1H), 8.75 (d, J = 8.3 Hz, 1H), 8.71 – 8.65 (m, 2H), 8.22 (ddd, J = 8.1, 2.3, 1.1 Hz, 1H), 8.04 – 7.95 (m, 2H), 7.83 – 7.74 (m, 2H), 7.63 (t, J = 7.9 Hz, 1H), 3.93 (s, 3H). ^{13}C NMR (151 MHz, DMSO) δ 166.3, 158.4, 155.3, 151.1, 149.7, 144.9, 139.4, 134.3, 130.1, 129.2, 128.5, 128.2, 126.9, 124.8, 124.0, 123.7,

123.0, 114.7, 52.5. Anal. Calcd. for $C_{21}H_{16}N_4O_2$; C, 70.77; H, 4.53; N, 15.72. Found: C, 70.92; H, 4.63; N, 15.72.

tert-Butyl 3-((2-(pyridin-4-yl)quinazolin-4-yl)amino)benzoate (39).

The compound was synthesized from **6** (242 mg, 1 mmol) and methyl tert-butyl 3-aminobenzoate (193 mg, 1 mmol) as described in the general procedure for compounds **11-41** to yield **39** as a yellow solid (255 mg, 64%), mp >300 °C. ^{1}H NMR (600 MHz, DMSO-d_6) δ 10.20 (s, 1H), 8.81 – 8.74 (m, 2H), 8.68 – 8.61 (m, 1H), 8.34 – 8.26 (m, 2H), 8.18 – 8.09 (m, 2H), 8.05 – 7.99 (m, 2H), 7.99 – 7.91 (m, 2H), 7.72 (ddd, J = 8.2, 5.8, 2.4 Hz, 1H), 1.57 (s, 9H). ^{13}C NMR (151 MHz, DMSO) δ 164.8, 158.1, 157.3, 150.5, 150.4, 145.4, 143.5, 133.9, 130.0, 128.6, 127.3, 126.1, 123.4, 121.9, 121.3, 114.7, 80.5, 28.1. Anal. Calcd. for $C_{24}H_{22}N_4O_2$; C, 72.34; H, 5.57; N, 14.06. Found: C, 72.50; H, 5.88; N, 13.99.

3-((2-(Pyridin-3-yl)quinazolin-4-yl)amino)benzoic acid (40).

The compound was synthesized from **6** (242 mg, 1 mmol) and methyl 3-aminobenzoic acid (137 mg, 1 mmol) as described in the general procedure for compounds **11-41** to yield **40** as a yellow-beige solid (147 mg, 43%), mp >300 °C. ^{1}H NMR (500 MHz, DMSO-d_6) δ 13.07 (s, 1H), 10.48 (s, 1H), 9.11 – 8.88 (m, 2H), 8.84 (t, J = 1.9 Hz, 1H), 8.81 – 8.61 (m, 3H), 8.20 (ddd, J = 8.2, 2.3, 1.1 Hz, 1H), 8.11 – 7.90 (m, 2H), 7.90 – 7.68 (m, 2H), 7.62 (t, J = 7.9 Hz, 1H). ^{13}C NMR (126 MHz, DMSO) δ 167.3, 158.5, 155.4, 150.8, 149.6, 145.1, 139.2, 134.2, 131.3, 129.0, 128.4, 128.1, 126.5, 124.9, 124.0, 123.6, 123.4, 114.7. Anal. Calcd. for $C_{20}H_{14}N_4O_2$; C, 70.17; H, 4.12; N, 16.37. Found: C, 70.27; H, 4.44; N, 16.45.

4-((2-(Pyridin-3-yl)quinazolin-4-yl)amino)benzoic acid (41).

The compound was synthesized from **6** (242 mg, 1 mmol) and methyl 4-aminobenzoic acid (137 mg, 1 mmol) as described in the general procedure for compounds **11-41** to yield **41** as a brown-beiges solid (188 mg, 55%), mp >300 °C. ^{1}H NMR (500 MHz, DMSO-d_6) δ 12.51 (s, 1H), 10.52 (s, 1H), 9.03 – 8.95 (m, 2H), 8.78 (dd, J = 8.3, 1.1 Hz, 1H), 8.74 – 8.68 (m, 2H), 8.16 – 8.09 (m, 2H), 8.08 – 8.03 (m, 2H), 8.03 – 7.95 (m, 2H), 7.77 (ddd, J = 8.2, 6.1, 2.1 Hz, 1H).^{13}C NMR (126 MHz, DMSO) δ 167.1, 158.4, 155.2, 151.5, 149.8, 144.3, 143.1, 134.3, 130.2, 128.5, 128.2, 125.9, 124.3, 123.8, 121.8, 114.8. Anal. Calcd. for $C_{20}H_{14}N_4O_2$; C, 70.17; H, 4.12; N, 16.37. Found: C, 70.49; H, 4.38; N, 16.25.

General Procedure for the Preparation of the 2-Substituted 6-Methyl-4-anilinopyrimidines 42-48.

To the corresponding 2-substituted 6-methyl-4-chloropyrimidine derivatives **9** and **10** (1 mmol) isopropanol (5 mL) was added together with the corresponding substituted aniline (1 mmol) and sealed in a microwave tube. The mixture was heated by 100 watt microwave irradiation to 110 °C for a period of 15 – 30 min until completion of the reaction as indicated by TLC. The formed precipitate was filtered off, washed with 10 mL isopropanol and dried in vacuo. If no precipitate was formed, the solvent was removed under reduced pressure and the remaining solid recrystallized from acetone.

3-((6-Methyl-2-(pyridin-4-yl)pyrimidin-4-yl)amino)benzonitrile (42). The compound was synthesized from **9** (206 mg, 1 mmol) and methyl 3-aminobenzonitrile (118 mg, 1 mmol) as described in the general procedure for compounds **42-48** to yield **42** as a white solid (135 mg, 47%), mp >300 °C. ^{1}H NMR (600 MHz, DMSO-d_6) δ 9.97 (s, 1H), 8.73 (d, J = 4.8 Hz, 2H), 8.21 (t, J = 1.9 Hz, 1H), 8.18 – 8.10 (m, 2H), 8.07 – 7.95 (m, 1H), 7.58 (t, J = 8.0 Hz, 1H), 7.47 (dt, J = 7.7, 1.2 Hz, 1H), 6.69 (s, 1H), 2.43 (s, 3H). ^{13}C NMR (151 MHz, DMSO) δ 165.9,

160.8, 160.6, 150.4, 145.1, 140.8, 130.4, 125.7, 124.3, 122.5, 121.7, 119.0, 111.8, 105.5, 23.9. Anal. Calcd. for $C_{17}H_{13}N_5$; C, 71.06; H, 4.56; N, 24.37. Found: C, 71.17; H, 4.37; N, 24.07.

N-(3-Methoxyphenyl)-6-methyl-2-(pyridin-4-yl)pyrimidin-4-amine (43). The compound was synthesized from **9** (206 mg, 1 mmol) and methyl 3-methoxyaniline (123 mg, 1 mmol) as described in the general procedure for compounds **42-48** to yield **43** as a light beige solid (140 mg, 48%), mp 227-229 (decomp.). ^{1}H NMR (500 MHz, DMSO-d_6) δ 10.23 (s, 1H), 9.04 – 8.95 (m, 2H), 8.63 – 8.53 (m, 2H), 7.43 (t, J = 2.2 Hz, 1H), 7.34 – 7.23 (m, 2H), 6.85 (s, 1H), 6.66 (ddd, J = 7.6, 2.4, 1.3 Hz, 1H), 3.78 (s, 3H), 2.45 (s, 3H). ^{13}C NMR (126 MHz, DMSO) δ 164.6, 161.0, 159.8, 158.5, 144.4, 140.6, 129.8, 124.0, 112.6, 108.9, 106.1, 105.9, 55.2, 23.3. Anal. Calcd. for $C_{17}H_{16}N_4O$; C, 69.85; H, 5.52; N, 19.17. Found: C, 69.53; H, 5.71; N, 19.52.

N-(4-Methoxyphenyl)-6-methyl-2-(pyridin-4-yl)pyrimidin-4-amine (44). The compound was synthesized from **9** (206 mg, 1 mmol) and methyl 4-methoxyaniline (123 mg, 1 mmol) as described in the general procedure for compounds **42-48** to yield **44** as a light beige solid (114 mg, 39%), mp > 300 °C. ^{1}H NMR (500 MHz, DMSO-d_6) δ 9.59 (s, 1H), 8.81 – 8.76 (m, 2H), 8.29 – 8.24 (m, 2H), 7.58 (d, J = 8.4 Hz, 2H), 7.00 – 6.94 (m, 2H), 6.59 (d, J = 0.8 Hz, 1H), 3.76 (s, 3H), 2.39 (d, J = 0.7 Hz, 3H). ^{13}C NMR (126 MHz, DMSO) δ 148.8, 122.3, 114.3, 55.4, 23.6. Anal. Calcd. for $C_{17}H_{16}N_4O$; C, 69.85; H, 5.52; N, 19.17. Found: C, 69.53; H, 5.71; N, 19.52.

3-((6-Methyl-2-phenylpyrimidin-4-yl)amino)benzonitrile (45). The compound was synthesized from **10** (205 mg, 1 mmol) and methyl 3-aminobenzonitrile (118 mg, 1 mmol) as described in the general procedure for compounds **42-48** to yield **45** as a white solid (157 mg, 55%), mp 290-291 °C (decomp.). ^{1}H NMR (500 MHz, DMSO-d_6) δ 10.87 (s, 1H), 8.33 – 8.17 (m, 3H), 8.02 (d, J = 8.1 Hz, 1H), 7.69 – 7.47 (m, 5H), 6.83 (s, 1H), 2.52 (s, 3H). ^{13}C NMR

(126 MHz, DMSO) δ 160.9, 132.2, 130.5, 128.9, 128.4, 118.8, 111.9, 104.4. Anal. Calcd. for $C_{18}H_{14}N_4$; C, 75.50.85; H, 4.93; N, 19.57. Found: C, 75.82; H, 5.24; N, 19.38.

4-((6-Methyl-2-phenylpyrimidin-4-yl)amino)benzonitrile (46). The compound was synthesized from **10** (205 mg, 1 mmol) and methyl 4-aminobenzonitrile (118 mg, 1 mmol) as described in the general procedure for compounds **42-48** to yield **46** as a white solid (180 mg, 63%), mp 262-264 °C (decomp.).^{1}H NMR (600 MHz, DMSO-d_6) δ 11.41 (s, 1H), 8.36 – 8.22 (m, 2H), 8.02 (d, J = 8.4 Hz, 2H), 7.94 – 7.82 (m, 2H), 6.98 (s, 1H), 2.55 (s, 3H). ^{13}C NMR (151 MHz, DMSO) δ 161.2, 160.9, 133.8, 132.8, 129.4, 129.1, 121.3, 119.5, 26.0. Anal. Calcd. for $C_{18}H_{14}N_4$; C, 75.50.85; H, 4.93; N, 19.57. Found: C, 75.74; H, 5.22; N, 19.22.

4-((6-Methyl-2-phenylpyrimidin-4-yl)amino)-2-nitrophenol (47). The compound was synthesized from **10** (205 mg, 1 mmol) and methyl 4-amino-2-nitrophenol (154 mg, 1 mmol) as described in the general procedure for compounds **42-48** to yield **47** as a yellow solid (168 mg, 52%), mp 276-278 °C (decomp.).^{1}H NMR (600 MHz, DMSO-d_6) δ 11.07 (s, 1H), 8.61 (s, 1H), 8.35 – 8.25 (m, 2H), 7.76 (d, J = 8.9 Hz, 1H), 7.68 (t, J = 7.3 Hz, 1H), 7.61 (t, J = 7.6 Hz, 2H), 7.26 (d, J = 9.0 Hz, 1H), 6.82 (s, 1H), 2.53 (s, 3H). ^{13}C NMR (151 MHz, DMSO) δ 129.0, 128.8, 119.9. Anal. Calcd. for $C_{17}H_{14}N_4O_3$; C, 63.35; H, 4.38; N, 17.38. Found: C, 63.63; H, 4.73; N, 17.26.

6-Methyl-N,2-diphenylpyrimidin-4-amine (48). The compound was synthesized from **10** (205 mg, 1 mmol) and methyl aniline (93 mg, 1 mmol) as described in the general procedure for compounds **42-48** to yield **48** as a white solid (165 mg, 63%), mp 250-251 °C (decomp.).^{1}H NMR (500 MHz, DMSO-d_6) δ 11.09 (s, 1H), 8.32 – 8.19 (m, 2H), 7.86 – 7.64 (m, 3H), 7.62 (dd, J = 8.3, 6.6 Hz, 2H), 7.50 – 7.39 (m, 2H), 7.21 (t, J = 7.4 Hz, 1H), 6.86 (s, 1H), 2.54 (s, 3H). ^{13}C NMR (126 MHz, DMSO) δ 161.0, 159.8, 137.9, 132.8, 129.2, 129.0,

128.7, 125.0, 121.9, 104.0, 20.1. Anal. Calcd. for $C_{17}H_{15}N_3$; C, 78.13; H, 5.79; N, 16.08. Found: C, 78.05; H, 5.63; N, 16.00.

Biological Investigations: Materials for Biological Investigation. Compound **55** ((3S,6S,12aS)-1,2,3,4,6,7,12,12a-Octahydro-9-methoxy-6-(2-methylpropyl)-1,4-dioxopyrazino[1′,2′:1,6]pyrido[3,4-b]indole-3-propanoicacid1,1-dimethylethyl ester) was purchased from Tocris Bioscience (Bristol, United Kingdom). All other chemicals were purchased from Sigma-Aldrich (Taufkirchen, Germany).

Cell based assays were carried out with 10 mM stock solutions of the test compound in DMSO. Krebs-HEPES buffer (KHB) was prepared from a solution of 118.6 mM NaCl, 4.7 mM KCl, 1.2 mM $MgSO_4$, 2.5 mM CaCl, 11.7 mM D-glucose monohydrate, and 10.0 mM HEPES in doubly distilled water. The pH of the solution was adjusted with 4 N NaOH (aq) at 37 °C and it was sterilized, using a 0.2 μM membrane filter.

Cell Culture. MDCK II BCRP cells were generated by transfection of the canine kidney epithelial cell line MDCK II with human wild-type cDNA C-terminally linked to the cDNA of the green fluorescent protein (GFP) and were a kind gift of Dr. A. Schinkel (The Netherlands Cancer Institute, Amsterdam, The Netherlands).[38] Cell culture was performed with Dulbecco's modified Eagle's medium (DMEM) containing 10% fetal calf serum (FCS), 50 μg/mL streptomycin, 50 U/mL penicillin G and 2 mM *L*-glutamine. Human ovarian carcinoma cell line A2780adr was purchased from European Collection of Animal Cell Culture (ECACC, No 93112520). The cell line shows an overexpression of ABCB1 and resistance against doxorubicin. Culture of these cells was carried out with RPMI-1640 medium supplemented with 20% FCS, 50 μg/mL streptomycin, 50 U/mL penicillin G and 2 mM *L*-glutamine. To ensure the overexpression of ABCB1, treatment with doxorubicin was carried out every 10 passages for less than 40 passages. The small cell lung cancer cell line

H69 AR with overexpression of ABCC1 was purchased from American Type Culture Collection (ATCC, CRL-11351). Culture of the cells was carried out in RPMI-1640 medium with 20% FCS, 50 mg/mL streptomycin, 50 U/mL penicillin G and 2 mM *L*-glutamine and kept under a 5% CO_2 humidified atmosphere at 37 °C. Subculturing of cells was performed with 0.05% Trypsin and 0.02% EDTA after reaching a confluence of 80-90%. Excess medium was removed from the cells by washing with PBS before trypsination. After detachment of the cells, they were centrifuged in a 50 mL falcon (266 x g, 4 °C, 4 min). The supernatant was removed by suction and the remaining cell pellet resuspended in fresh medium. The cell count for all cells was determined with a CASY1 model TT cell counter equipped with a 150 µm capillary (Schaerfe System GmbH, Reutlingen, Germany). To remove remaining liquids, all cells were washed with KHB three times before using them in cell based assays.

Hoechst 33342 Accumulation Assay. The Hoechst 33342 accumulation assay was performed to investigate the inhibitory effect on ABCG2, as described earlier with small modifications.[39, 40, 41, 42, 43, 44, 45, 46, 47, 48, 49, 50] Stock-solutions were prepared by dissolving the test compound in DMSO at a final concentration of 10 mM. Sterile filtered KHB, a small amount of methanol together with the stock solution were used to prepare various dilutions of the corresponding compound. The amount of methanol and DMSO in the final concentration was chosen not to exceed 5% and 0.1%, respectively.

Cells were harvested after reaching a confluence of 80-90% by gentle trypsination (0.05% trypsin/0.02% EDTA) and were centrifuged (266 x g, 4 °C, 4 min) to obtain a cell pellet. The cell pellet was resuspended in fresh medium and the cell density determined with a CASY1 model TT cell counter device. Residual medium was removed by centrifugation of the cell suspension three times in KHB.

The assay was carried out with 90 µL of the washed cell suspension together with 10 µL of different compound dilutions to obtain a cell density of approximately 30,000 cells in each well (96 well plate, Greiner, Frickenhausen, Germany). Following with a pre-incubation period of 30 min at 37 °C and 5% CO_2, 20 µL of a 6 µM Hoechst 33342 solution (protected from light) was quickly added to each well giving a final concentration of 1 µM Hoechst 33342. Measurement of the fluorescence was performed immediately in constant time intervals (60 s) up to 120 min with an excitation wavelength of 355 nm and an emission wavelength of 460 nm using a BMG POLARstar microplate reader (BMG Labtech, Offenburg, Germany). For the analysis of the data, fluorescence of the wells containing only compound in KHB was subtracted from the fluorescence reading obtained from the MDCK II cells to correct for potential fluorescence of the compound. Average of the fluorescence measured between 100 and 109 min (steady state) was calculated for each concentration and plotted against the logarithm of the compound concentration. Concentration-response curves were fitted by nonlinear regression using the four-parameter logistic equation with variable Hill slope, or the three-parameter logistic equation with a fixed Hill slope of one, whatever equation was statistically preferred (GraphPad Prism, version 5.0, San Diego, CA, USA). From the pIC_{50} values and their standard deviation IC_{50} values and standard deviations were calculated according to the equation for log-normal distributed values.[51,52]

Calcein AM Assay. Selectivity of the test compounds toward ABCG2 was determined by checking the inhibitory activity against ABCB1 and ABCC1 in the calcein AM assay described earlier.[40,41,42,43,44,45,46,47,48,50,53,54,55,56] For the assay the ABCB1 overexpressing cell line A2780adr and the ABCC1 overexpressing cell line H69AR were used. Cells were harvested at a confluence of 80-90% and prepared as described above for the MDCK II cells. After washing the cells three times with KHB a 90 µL suspension cotaining approximately

30,000 cells was seeded in each well of a colourless flat bottom 96 well plate (Greiner), along with 10 µL of different compound dilutions. Subsequently the prepared plates were kept at 5% CO_2 and 37 °C for a period of 30 min. After this preincubation, 33 µL of a 1.25 µM calcein AM solution (protected from light) was quickly added to each well and fluorescence measured immediately in a 37 °C tempered BMG POLARstar microplate reader. Fluorescence was then measured over a period of 60 min in constant time intervals (60 s) using an excitation wavelength of 485 nm and an emission wavelength of 520 nm. From the initial linear part of the obtained fluorescence time curve the slope for each concentration was calculated. Thereby a slope concentration response curve was obtained that was fitted by nonlinear regression, using the four-parameter logistic equation with variable Hill slope, or the three-parameter logistic equation with a Hill slope of one, whatever equation was statistically preferred. From the pIC_{50} values and their standard deviation IC_{50} values and standard deviations were calculated according to the equation for log-normal distributed values.[51,52]

MTT Viability Assay. Intrinsic cytotoxicity of selected compounds was investigated using the MTT viability assay as described earlier with slight modifications. [30, 41, 44, 45, 46, 47, 50, 56] MDCK II BCRP and parental cells were seeded in 96 well tissue culture plates (Sarsted, Newton, USA) at a density of approximately 2,000 cells per well in a volume of 180 µL culture medium and kept under 5% CO_2 and 37 °C for 12 h. The old medium was removed from the plate with the completely attached cells and quickly replaced with 180 µL of fresh medium. Then, 20 µL of different compound dilutions in culture medium was added to each well to a final volume of 200 µL and plates were stored at 5% CO_2 and 37 °C for 72 h. The content of methanol and DMSO was chosen not to exceed 1.8% and 1% in the highest concentration, respectively. Toxic effects caused by the DMSO and methanol content, used for the compound dilutions, was determined by an additional dilution without compound.

Moreover, a positive control with medium and 10% (v/v) DMSO and a negative control of only medium were carried out. After a 72 h period of incubation, 40 µL of MTT reagent (3-(4,5-dimethylthiazol-2-yl)-2,5-diphenyltetrazolium bromide) was added to each well and the plate incubated for one hour. After removing the supernatants 100 µL of DMSO to each well resulting in lysis of the cells and solubilisation of the formed formazan. Absorbance was determined spectrophotometrically at 544 nm and background correction at 710 nm using a BMG POLARstar microplate reader. Concentration-response curves were fitted by nonlinear regression using the four-parameter logistic equation with variable Hill slope, or the three-parameter logistic equation with a fixed Hill slope of one, whatever equation was statistically preferred (GraphPad Prism, version 5.0, San Diego, CA, USA). From the pIC_{50} values and their standard deviation IC_{50} values and standard deviations were calculated according to the equation for log-normal distributed values.[51,52]

MDR Reversal Assay. The ability to reverse resistance of ABCG2 expressing MDCK II cells toward cytotoxic substrates like SN-38 was tested for compounds **14**, **16** and **47**. For this purpose 160 µL of a cell suspension of MDCK II BCRP and parental cells in culture medium was added to each well of a clear 96 well tissue culture plate (Sarsted, Newton, USA), resulting in a cell density of approximately 2,000 cells per well. The plate was stored under 5% CO_2 at 37 °C for 12 h. After incubation the culture medium was replaced as described above. Then, 20 µL of different compound dilutions in culture medium were added to each row. Colum wise, 20 µL of different dilutions of SN-38 were added to a final volume of 200 µL. A positive control was established using parental MDCK II cells without adding a modulator as well as a negative control by adding 10% (v/v) of DMSO to a well. After 72 h of incubation the plates were prepared and measured as described above.

Regarding the MTT assay with MX, plates were prepared with cells as described above. After replacement of the medium with fresh culture medium, 20 µL of different compound dilutions

were added to the rows. Additionally, 20 µL of 5 µM MX and culture medium were added in alternating order to the rows, respectively, to a final volume of 200 µL. For comparison, complete cell death was induced by adding 10% (v/v) of DMSO to some wells. The preparation of the plate with subsequent measurement and data analysis was carried out as described above.

Protein Expression in Insect Cells and ATPase Measurements of ABCG2 Membranes.

High Five ™ insect cells were seeded in culture flasks with Express Five® medium and were incubated at 27°C. After a few passages when cells were healthy and homogenous, cells were counted and about 20 million cells per flask were seeded for baculovirus infection with Autographa californica multicapsid nuclear polyhedrosis virus (AcMNPV). Cells were harvested 72 hours after infection, centrifuged and afterwards membrane preparation was performed.[45] Two ml of membrane preparation homogenization buffer (50 mM Tris pH 7.5, 2 mM EGTA pH 7.0, 50 mM Mannitol, 2 mM DTT, 1 mM PMSF, 2 µM pepstatin, 1 µM leupeptin, 1 mM benzamidine) was used for 20 million cells. Cells were disrupted by a dounce homogenizer. Cellular debris was pelleted by centrifugation at 500 × g for 10 min at 4 °C and was discarded. The supernatant was centrifuged at 300,000 × g for 30 min at 4 °C to obtain a pellet of enriched plasma membranes. Finally membranes were resuspended in 100 µl resuspension buffer (50 mM Tris pH 7.5, 1 mM EGTA at pH 7.0, 10% (v/v) glycerol, 0.3 M mannitol, 1 mM DTT, 1 mM PMSF, 2 µM pepstatin, 1 µM leupeptin, 1 mM benzamidine) per flask and were frozen and stored at −80 °C. ATPase activity measurements of selected compounds was performed by a colorimetric ascorbic acid ammonia molybdate reaction.[57] Vanadate-sensitive basal ATPase activity was compared to vanadate-sensitive drug-stimulated or inhibited activity. Compound **55** was used as standard for ATPase inhibition, quercetin was used as positive control with high stimulation of ABCG2 transport activity. Investigated compounds were dissolved in DMSO, final concentration of DMSO was 1%,

which showed no observable effect on basal ATPase activity. All measurements were repeated at least three times. Concentration-response curves were fitted by nonlinear regression using the three-parameter logistic equation with a fixed Hill slope of one (GraphPad Prism, version 5.0, San Diego, CA, USA). In case of biphasic curves a two-site binding model was used to determine K_m and K_i.[58]

Inhibition Kinetics. For more detailed information about the type of interaction with the substrate Hoechst 33342, we performed extended enzyme kinetic experiments with selected compounds. The experiments were carried out with various concentrations of selected compounds as well as of Hoechst 33342. For determination of the interaction type, we utilized the Lineweaver-Burk linearization technique, the half reciprocal plot according to Hanes-Woolf and the direct linear plot according to Cornish-Bowden to confirm our results. The Hoechst 33342 assay was performed as described above, except that the concentration of Hoechst 33342 varied in the range of 0.4 µM to 2.4 µM, whereas the concentration of compounds was adjusted to the corresponding IC_{50} value. Response in absence of investigated compounds was used as control.

Associated Content

Supporting Information

SMILES and logP values with the corresponding biological data (csv).

Author Information

Corresponding Author

* Phone: +49-228-735213. E-mail: mwiese@uni-bonn.de

ORCID

Michael Wiese 0000-0002-5851-5336

Acknowledgments

We would like to thank Dr. A. Schinkel (The Netherlands Cancer Institute, Amsterdam, The Netherlands) for kindly providing the MDCK II ABCG2 expressing cell line. We also thank O. Laufkötter for providing the image used for the TOC graphic.

Abbreviations Used

ABC, ATP-binding cassette; BCRP, breast cancer resistance protein (ABCG2); CsA, cyclosporine A; DMEM, Dulbecco's modified Eagle's medium; FCS, fetal calf serum; FTC, fumitremorgin C; GI_{50}, half-maximal growth inhibition; GFP, green fluorescent protein; HEPES, 4-(2-hydroxyethyl)-1-piperazineethanesulfonic acid; IC_{50}, half-maximal inhibitory concentration; KHB, Krebs-HEPES buffer; MDCK, Madin Darby Canine Kidney; MDR, multidrug resistance; MRP1, multidrug resistance-associated protein 1 (ABCC1); MTT, 3-(4,5-dimethylthiazol-2-yl)-2,5-diphenyltetrazolium bromide; MX, mitoxantrone; NBD, nucleotid binding domain; P-gp, P-glycoprotein (ABCB1)

References

(1) Robey, R. W.; To, K. K.; Polgar, O.; Dohse, M.; Fetsch, P.; Dean, M.; Bates, S. E. ABCG2: A Perspective. *Adv. Drug Delivery Rev.* **2009**, *61*, 3-13.

(2) Mo, W.; Zhang, J.-T. Human ABCG2: Structure, Function, and its Role in Multidrug Resistance. *Int. J. Biochem. Mol. Biol.* **2012**, *1*, 1-27.

(3) Zhang J. T. Use of Arrays to Investigate the Contribution of ATP-Binding Cassette Transporters to Drug Resistance in Cancer Chemotherapy and Prediction of Chemosensitivity. *Cell Res.* **2007**, *17*, 311-323.

(4) Gottesman, M. M.; Fojo, T.; Bates, S. E. Multidrug Resistance in Cancer: Role of ATP-dependent Transporters. *Nat. Rev. Cancer* **2002**, *2*, 48–58.

(5) Miyake, K.; Mickley, L.; Litman, T.; Zhan, Z.; Robey, R.; Cristensen, B.; Brangi, M.; Greenberger, L.; Dean, M.; Fojo, T.; Bates, S. E. Molecular Cloning of cDNAs Which are Highly Overexpressed in Mitoxantrone Resistant Cells: Demonstration of Homology to ABC Transport Genes. *Cancer Res.* **1999**, *59*, 8–13.

(6) Pluchino, K. M.; Hall, M. D.; Goldsborough A. S.; Callaghan, R.; Gottesman, M. M. Collateral Sensitivity as a Strategy Against Cancer Multidrug Resistance. *Drug Resist. Updates* ***2012***, *15*, 98-105.

(7) Fojo, A. T.; Ueda, K.; Slamon, D. J.; Poplack, D. G.; Gottesman, M. M.; Pastan, I. Expression of a Multidrug-resistance Gene in Human Tumors and Tissues. *Proc. Natl. Acad. Sci. U. S. A.* **1987**, *84*, 265–269.

(8) McDevitt, C. A.; Collins, R.; Kerr, I. D.; Callaghan, R. Purification and Structural Analyses of ABCG2. *Adv. Drug Delivery Rev.* **2009**, *61*, 57–65.

(9) Ricci, J. W. ABCG2 Inhibitors: Will They Find Clinical Relevance? *J. Dev. Drugs* **2015**, *4*, 1-6.

(10) Diestra, J. E.; Scheffer, G. L.; Català, I.; Maliepaard, M.; Schellens, J. H.; Scheper, R. J.; Germà-Lluch, J. R.; Izquierdo, M, A. Frequent Expression of the Multi-drug Resistance-associated Protein BCRP/MXR/ABCP/ABCG2 in Human Tumours Detected by the BXP-21 Monoclonal Antibody in Paraffin-Embedded Material. *J. Pathol.* **2002**, *198*, 213-219.

(11) Rosenberg, M. F.; Bikadi, Z.; Chan, J.; Liu, X.; Ni, Z.; Cai, X.; Ford, R. C.; Mao, Q. The Human Breast Cancer Resistance Protein (BCRP/ABCG2) Shows Conformational Changes with Mitoxantrone. *Structure* **2010**, *18*, 482-493.

(12) Wong, K.; Briddon, S. J.; Holliday, N. D.; Kerr, I. D. Plasma Membrane Dynamics and Tetrameric Organisation of ABCG2 Transporters in Mammalian Cells Revealed by Single Particle Imaging Techniques. *Biochim. Biophys. Acta* **2016**, *1863*, 19-29.

(13) Dezi, M.; Fribourg, P.-F.; Di Cicco, A.; Arnaud, O.; Marco, S.; Falson, P.; Di Pietro, A.; Lévy, D. The Multidrug Resistance Half-transporter ABCG2 is Purified as a Tetramer Upon Selective Extraction from Membranes. *Biochim. Biophys. Acta* **2010**, *1798*, 2094-2101.

(14) McDevitt, C. A.; Collins, R. F.; Conway, M.; Modok, S.; Storm, J.; Kerr, I. D.; Ford, R. C.; Callaghan, R. Purification and 3D Structural Analysis of Oligomeric Human Multidrug Transporter ABCG2. *Structure* **2006**, *14*, 1623–1632

(15) Xu, J.; Liu, Y.; Yang, Y; Bates, S.; Zhang, J.-T. Characterization of Oligomeric Human Half-ABC Transporter ATP-binding Cassette G2. *J. Biol. Chem.* **2004**, *19*, 19781–19789.

(16) Lee, J. Y.; Kinch, L. N.; Borek, D. M.; Wang, J.; Wang, J.; Urbatsch, I. L.; Xie, X. S.; Grishin, N. V.; Cohen, J. C.; Otwinowski, Z.; Hobbs, H. H.; Rosenbaum, D. M. Crystal structure of the human sterol transporter ABCG5/ABCG8. *Nature* **2016**, *533*, 561-564.

(17) László, L.; Sarkadi, B.; Hegedűs, T. Jump into a New Fold-A Homology Based Model for the ABCG2/BCRP Multidrug Transporter. *PLoS One* **2016**, *11*, 1-22.

(18) Doyle, A.; Ross, D. D. Multidrug Resistance Mediated by the Breast Cancer Resistance Protein BCRP (ABCG2). *Oncogene* **2003**, *22*, 7340–7358.

(19) Stacy, A. E. Molecular Pharmacology of ABCG2 and its Role in Chemoresistance. *Mol. Pharmacol.* **2013**, *84*, 655-669.

(20) Juvale, K.; Wiese, M. Design of Inhibitors of BCRP/ABCG2. *Future Med. Chem.* **2015**, *7*, 1521-1527.

(21) Wang, X.; Xia, B.; Liang, Y.; Peng, L.; Wang, Z.; Zhou, J.; Wang, W.; Jiang, B. Membranous ABCG2 Expression in Colorectal Cancer Independently Correlates with Shortened Patient Survival. *Cancer Biomarkers* **2013***, 13*, 81-88.

(22) Lin, P. C.; Lin H. H.; Lin, J. K.; Lin, C. C.; Yang, S. H.; Li, A. F.; Chen, W. S.; Chang, S. C. Expression of ABCG2 Associated with Tumor Response in Metastatic Colorectal Cancer Patients Receiving First-Line FOLFOX Therapy - Preliminary Evidence. *Int. J. Biol. Markers* **2013**, *28*, 182-186.

(23) Szakács, G.; Hall, M. D.; Gottesman, M. M.; Boumendjel, A.; Kachadourian, R.; Day, B. J.; Baubichon-Cortay, H.; Di Pietro, A. Targeting the Achilles Heel of Multidrug-resistant Cancer by Exploiting the Fitness Cost of Resistance. *Chem. Rev.* **2014**, *114*, 5753−5774.

(24) Rabindran, S. K.; He, H.; Singh, M.; Brown, E.; Collins, K. I.; Annable, I.; Greenberger, L. M. Reversal of a Novel Multidrug Resistance Mechanism in Human Colon Carcinoma Cells by Fumitremorgin C. *Cancer Res.* **1998**, *58*, 5850–5858.

(25) Allen, J. D.; van Loevezijn, A.; Lakhai, J. M.; van der Valk, M.; van Tellingen, O.; Reid, G.; Schellens, J. H.; Koomen, G. J.; Schinkel, A. H. Potent and Specific Inhibition of the Breast Cancer Resistance Protein Multidrug Transporter in Vitro and in Mouse Intestine by a Novel Analogue of Fumitremorgin C. *Mol. Cancer Ther.* **2002**, *1*, 417–425.

(26) Weidner, L. D.; Zoghbi, S. S.; Lu, S.; Shukla, S.; Ambudkar, S. V.; Pike, V. W.; Mulder, J.; Gottesman, M. M.; Innis, R. B.; Hall, M. D.; The Inhibitor Ko143 Is Not Specific for ABCG2. *J. Pharm. Exp. Ther.* **2015**, *354*, 384-393.

(27) Gozzi, G. J.; Bouaziz, Z.; Winter, E.; Daflon-Yunes, N.; Honorat, M.; Guragossian, N.; Marminon, C.; Valdameri, G.; Bollacke, A.; Guillon, J.; Pinaud, N.; Marchivie, M.; Cadena, S. M.; Jose, J.; Le Borgne, M.; Di Pietro, A. Phenolic Indeno[1,2-b]indoles as

ABCG2-selective Potent and Non-toxic Inhibitors Stimulating Basal ATPase Activity. *Drug Des., Dev. Ther.* **2015**, *9*, 3481-3495.

(28) Pires Ado, R.; Lecerf-Schmidt, F.; Guragossian, N.; Pazinato, J.; Gozzi, G. J.; Winter, E.; Valdameri, G.; Veale, A.; Boumendjel, A.; Di Pietro, A.; Pérès, B. New, Highly Potent and Non-toxic, Chromone Inhibitors of the Human Breast Cancer Resistance Protein ABCG2. *Eur. J. Med. Chem.* **2016**, *122*, 291-301.

(29) Pick, A.; Wiese, M. Tyrosine Kinase Inhibitors Influence ABCG2 Expression in EGFR-positive MDCK BCRP Cells Via the PI3K/Akt Signaling Pathway. *ChemMedChem* **2012**, *7*, 650-662.

(30) Juvale, K.; Wiese, M. 4-Substituted-2-phenylquinazolines as Inhibitors of BCRP. *Bioorg. Med. Chem. Lett.* **2012**, *22*, 6766−6769.

(31) Juvale, K.; Gallus, J.; Wiese, M. Investigation of Quinazolines as Inhibitors of Breast Cancer Resistance Protein (ABCG2). *Bioorg. Med. Chem.* **2013**, *21*, 7858-7873.

(32) Krapf, M. K.; Wiese, M. Synthesis and Biological Evaluation of 4-Anilino-quinazolines and -quinolines as Inhibitors of Breast Cancer Resistance Protein (ABCG2). *J. Med. Chem.* **2016**, *59*, 5449-5461.

(33) Tawar, U.; Jain, A. K.; Dwarakanath, B. S.; Chandra, R.; Singh, Y.; Chaudhury, N. K.; Khaitan, D.; Tandon, V. Influence of Phenyl Ring Disubstitution on Bisbenzimidazole and Terbenzimidazole Cytotoxicity: Synthesis and Biological Evaluation as Radioprotectors. *J. Med. Chem.* **2003**, *46*, 3785–3792.

(34) Litman, T.; Nielsen D.; Skovsgaard T.; Zeuthen T.; Stein W. D. ATPase Activity of P-glycoprotein Related to Emergence of Drug Resistance in Ehrlich Ascites Tumor Cell-lines. *Biochim. Biophys. Acta* **1997**, *1361*, 147-158.

(35) Buxbaum E. Co-operating ATP Sites in the Multiple Drug Resistance Transporter Mdr1. *Eur. J. Biochem.* **1999**, *265*, 54 - 63.

(36) Egido, E.; Müller, R.; Li-Blatter, X.; Merino, G.; Seelig, A. Predicting Activators and Inhibitors of the Breast Cancer Resistance Protein (ABCG2) and P□Glycoprotein (ABCB1) Based on Mechanistic Considerations. *Mol. Pharm.* **2015**, *12*, 4026-4037.

(37) Kraege, S.; Stefan, K.; Juvale, K.; Ross, T.; Willmes, T.; Wiese, M. The Combination of Quinazoline and Chalcone Moieties Leads to Novel Potent Heterodimeric Modulators of Breast Cancer Resistance Protein (BCRP/ABCG2). *Eur. J. Med. Chem.* **2016**, *117*, 212-229.

(38) Pavek, P.; Merino, G. Wagenaar, E.; Bolscher, E.; Novotna, M.; Jonker, J. W.; Schinkel, A. H. Human Breast Cancer Resistance Protein: Interactions with Steroid Drugs, Hormones, the Dietary Carcinogen 2-Amino-1-methyl-6-phenylimidazo(4,5-b)pyridine, and Transport of Cimetidine. *J. Pharmacol. Exp. Ther.* **2005**, *312*, 144–152.

(39) Pick A.; Müller, H.; Wiese, M. Structure-activity Relationships of New Inhibitors of Breast Cancer Resistance Protein (ABCG2). *Bioorg. Med. Chem.* **2008**, *16*, 8224–8236.

(40) Pick, A.; Klinkhammer, W.; Wiese, M. Specific Inhibitors of the Breast Cancer Resistance Protein (BCRP). *ChemMedChem* **2010**, *5*, 1498–1505.

(41) Marighetti, F.; Steggemann, K.; Hanl, M.; Wiese, M. Synthesis and Quantitative Structure-activity Relationships of Selective BCRP Inhibitors. *ChemMedChem* **2013**, *8*, 125–135.

(42) Pick, A.; Müller, H.; Mayer, R.; Haenisch, B.; Pajeva, I. K.; Weigt, M.; Bonisch, H.; Muller, C. E.; Wiese, M. Structure-activity Relationships of Flavonoids as Inhibitors of Breast Cancer Resistance Protein (BCRP). *Bioorg. Med. Chem.* **2011**, *19*, 2090−2102.

(43) Müller, H.; Klinkhammer, W.; Globisch, C.; Kassack, M. U.; Pajeva, I. K.; Wiese, M. New Functional Assay of P-glycoprotein Activity Using Hoechst 33342. *Bioorg. Med. Chem.* **2007**, *15*, 7470−7479.

(44) Juvale, K.; Pape, V. F.; Wiese, M. Investigation of Chalcones and Benzochalcones as Inhibitors of Breast Cancer Resistance Protein. *Bioorg. Med. Chem.* **2012**, *20*, 346-355.

(45) Gallus, J.; Juvale, K.; Wiese, M. Characterization of 3-Methoxy Flavones for their Interaction with ABCG2 as Suggested by ATPase Activity. *Biochim. Biophys. Acta* **2014**, *1838*, 2929-2938.

(46) Singh, M. S.; Juvale, K.; Wiese, M.; Lamprecht, A. Evaluation of Dual P-gp-BCRP Inhibitors as Nanoparticle Formulation. *Eur. J. Pharm. Sci.* **2015**, *77*, 1-8.

(47) Juvale, K.; Stefan, K.; Wiese, M. Synthesis and Biological Evaluation of Flavones and Benzoflavones as Inhibitors of BCRP/ABCG2. *Eur. J. Med. Chem.* **2013**, *67*, 115−126.

(48) Müller, H.; Pajeva, I. K.; Globisch, C.; Wiese, M. Functional Assay and Structure-activity Relationships of New Third-generation P-glycoprotein Inhibitors. *Bioorg. Med. Chem.* **2008**, *16*, 2456−2470.

(49) Pick, A.; Muller, H.; Wiese, M. Structure-activity Relationship of New Inhibitors of Breast Cancer Resistance Protein (ABCG2). *Bioorg. Med. Chem. Lett.* **2010**, *20*, 180−183.

(50) Köhler, S.; Wiese, M. HM30181 Derivatives as Novel Potent and Selective Inhibitors of the Breast Cancer Resistance Protein (BCRP/ABCG2). *J. Med. Chem.* **2015**, *58*, 3910−3921.

(51) https://en.wikipedia.org/wiki/Log-normal_distribution, last accessed on 3.10.2016

(52) http://de.mathworks.com/help/stats/lognstat.html, last accessed on 3.10.2016

(53) Leyers, S.; Häcker, H.-G.; Wiendlocha, J.; Gütschow, M.; Wiese, M. A 4-Aminobenzoic Acid Derivative as Novel Lead for Selective Inhibitors of Multidrug Resistance-associated Proteins, *Bioorg. Med. Chem. Lett.* **2008**, *18*, 4761-4763.

(54) Klinkhammer, W.; Müller, H.; Globisch, C.; Pajeva, I. K.; Wiese, M. Synthesis and Biological Evaluation of a Small Molecule Library of 3rd Generation Multidrug Resistance Modulators, *Bioorg. Med. Chem.* **2009**, *17*, 2524-2535.

(55) Häcker, H.-G.; Leyers, S.; Wiendlocha, J.; Gütschow, M.; Wiese, M. Aromatic 2-(Thio)ureidocarboxylic Acids As a New Family of Modulators of Multidrug Resistance-Associated Protein 1: Synthesis, Biological Evaluation, and Structure-Activity Relationships, *J. Med. Chem.* **2009**, *52*, 4586-4595.

(56) Marighetti, F.; Steggemann, K.; Karbaum, M.; Wiese, M. Scaffold Identification of a New Class of Potent and Selective BCRP-inhibitors. *ChemMedChem* **2015**, *10*, 742–751.

(57) Sarkadi, B.; Price, E. M.; Boucher R. C.; Germann U. A.; Scarborough G. A. Expression of the Human Multidrug Resistance cDNA in Insect Cells Generates a High Activity Drug-stimulated Membrane ATPase. *J. Biol. Chem.* **1992**, *267*, 4854-4858.

(58) Al-Shawi, M. K.; Polar, M. K.; Omote, H.; Figler, R. A. Transition State Analysis of the Coupling of Drug Transport to ATP Hydrolysis by P-glycoprotein. *J. Biol. Chem.* **2003**, *278*, 52629-52640.

Scheme 1. General Synthesis Route for the Compounds **1-48.**[a]

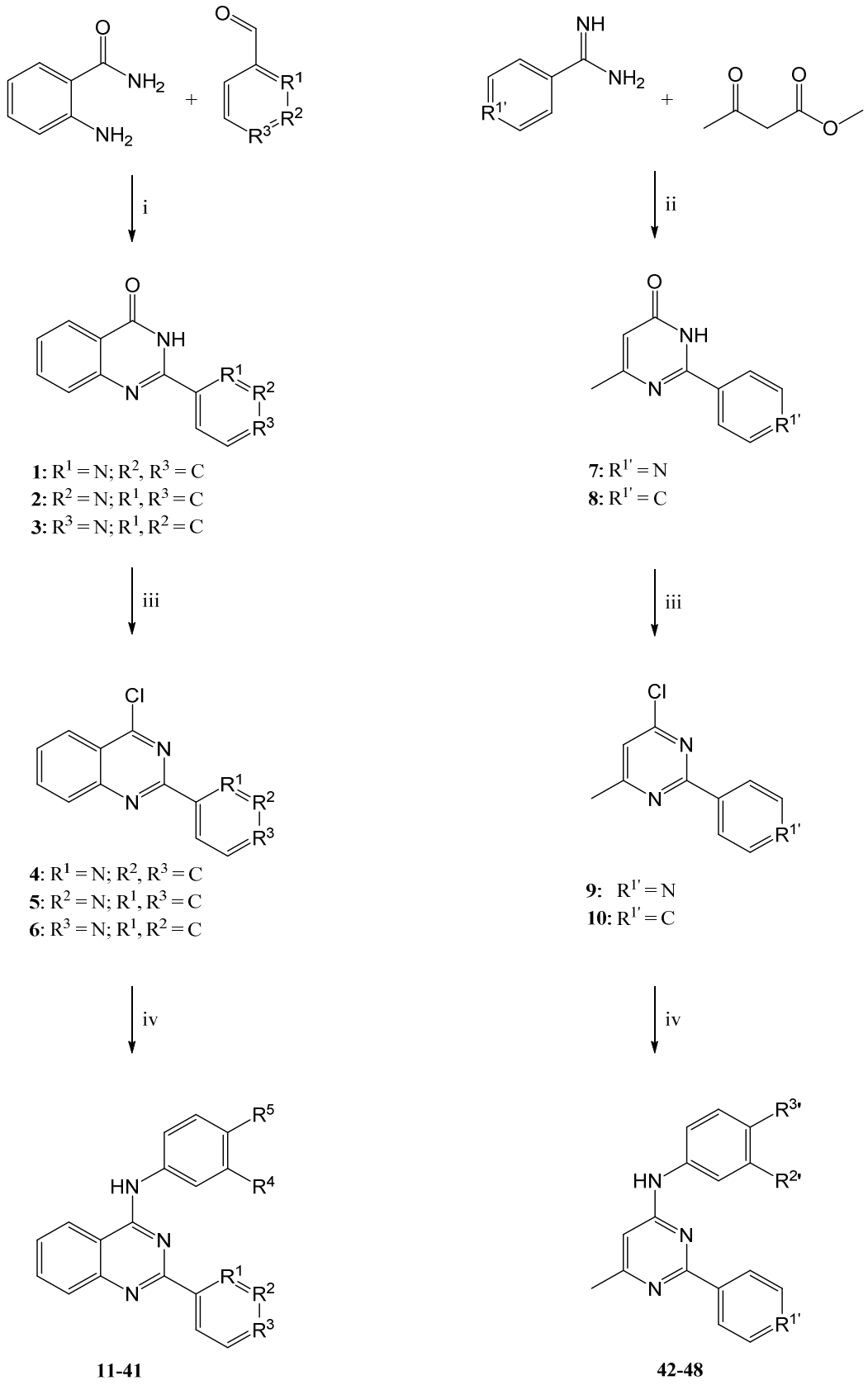

[a]: Reagents and conditions: (i) DMF, I_2, K_2CO_3, 70-90 °C, 4-8 h. (ii) MeOH, NaOMe, 60 watt microwave irradiation, 70 °C, 4 h. (iii) $POCl_3$, reflux, 4-12 h. (iv) Substituted aniline, 100 watt microwave irradiation, 110 °C, 15 - 30 min.

Table 1. Inhibitory Activities Determined in the Hoechst 33342 Accumulation Assay Using ABCG2 Overexpressing MDCK II Cells. Structural Formulas of Scaffold A and B are Depicted Below.

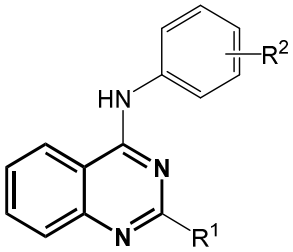

Scaffold A: Quinazoline

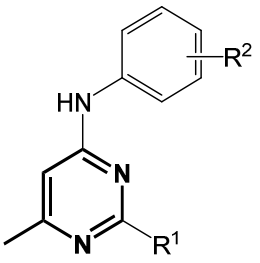

Scaffold B: 4-Methylpyrimidine

Compd.	R^1	R^2	Scaffold	Hoechst 33342 IC_{50} ± SD [nM][d]
11	2-Pyr	3-NO_2	A	376 ± 91
12	3-Pyr	3-NO_2	A	105 ± 35
13	4-Pyr	3-NO_2	A	117 ± 29
14	3-Pyr	4-NO_2	A	64.1 ± 8.5
15	2-Pyr	3-CN	A	507 ± 61
16	3-Pyr	3-CN	A	108 ± 21
17	4-Pyr	3-CN	A	134 ± 10
18	3-Pyr	4-CN	A	166 ± 29
19	2-Pyr	3-OMe	A	1630 ± 320
20	3-Pyr	3-OMe	A	1020 ± 180
21	4-Pyr	3-OMe	A	558 ± 111
22	4-Pyr	4-OMe	A	742 ± 21
23	2-Pyr	3,4-OMe	A	1060 ± 80
24	3-Pyr	3,4-OMe	A	753 ± 151
25	4-Pyr	3,4-OMe	A	545 ± 113
26	4-Pyr	3-CF_3	A	216 ± 40
27	4-Pyr	4-CF_3	A	488 ± 38
28	4-Pyr	3-CF_3,4-OMe	A	146 ± 23
29	3-Pyr	3-F	A	156 ± 37
30	4-Pyr	3-SO_2F	A	1380 ± 184
31	3-Pyr	3-$N(Me)_2$	A	1200 ± 210
32	4-Pyr	3-OH	A	1070 ± 190
33	4-Pyr	4-OH	A	4260 ± 1220
34	3-Pyr	3-CH_2OH	A	810 ±.239
35	4-Pyr	3-CH_2OH	A	921 ± 216
36	3-Pyr	3-NO_2,4-OH	A	245 ± 21
37	3-Pyr	3-CO_2Me	A	362 ± 74
38	4-Pyr	3-CO_2Me	A	405 ± 98
39	4-Pyr	3-CO_2tBu	A	299 ± 97

40	4-Pyr	3-CO_2H	A	60000 ± 14800
41	4-Pyr	4-CO_2H	A	9640 ± 2068
42	4-Pyr	3-CN	B	132 ± 24
43	4-Pyr	3-OMe	B	271 ± 28
44	4-Pyr	4-OMe	B	874 ± 181
45	Ph	3-CN	B	122 ± 24
46	Ph	4-CN	B	128 ± 32
47	Ph	3-NO_2,4-OH	B	98.8 ± 17.4
48	Ph	H	B	648 ± 149
49[a]	Ph	3-CN	A	140 ± 40
50[b]	Ph	4-CN	A	71.4 ± 10.1
51[b]	Ph	3-NO_2,4-OH	A	81.1. ± 9.2
52[b]	Ph	4-OH	A	211 ± 38
53[b]	Ph	3-F	A	363 ± 54
54[b]	Ph	H	A	882 ± 157
55[c]				227 ± 14

[a]: IC_{50} value taken from literature.[30]
[b]: Compounds synthesized in earlier study.[32]
[c]: Used as reference in the assay.
[d]: IC_{50} values are means of at least three independent experiments. Maximum inhibition compared to the standard compound **55** ranged between 80 and 110%.

Table 2. Inhibitory Activity of Compounds Exhibiting an Inhibition of more than 25% in Comparison to the Reference CsA in a Calcein AM Assay at 10 μM.

Compd.	R^1	R^2	Scaffold	Calcein AM (ABCB1) IC_{50} ± SD [μM][a]	Calcein AM (ABCC1) IC_{50} ± SD [μM][b]
19	2-Pyr	3-OMe	A	12.7 ± 1.8	
20	3-Pyr	3-OMe	A	4.78 ± 0.57	
21	4-Pyr	3-OMe	A	5.43 ± 0.83	
22	4-Pyr	4-OMe	A		17.9 ± 2.1
23	2-Pyr	3,4-OMe	A	6.30 ± 0.36	
24	3-Pyr	3,4-OMe	A	3.11 ± 0.21	
25	4-Pyr	3,4-OMe	A	2.08 ± 0.36	
28	4-Pyr	3-CF_3,4-OMe	A	2.78 ± 0.50	
38	4-Pyr	3-CO_2Me	A	6.37 ± 0.12	
39	4-Pyr	3-CO_2tBu	A	0.334 ± 0.056	
41	4-Pyr	4-CO_2H	A	3.67 ± 0.10	
47	Ph	3-NO_2,4-OH	B		15.9 ± 2.9
CsA[c]				1.21 ± 0.16	2.97 ± 0.38

[a]: The ABCB1 overexpressing cell line A2780adr was used.
[b]: The ABCC1 overexpressing cell line H69AR was used.
[c]: Cyclosporine A is used as reference for both assays.

Table 3. Intrinsic Toxicity of Selected Compounds toward MDCK II ABCG2 Overexpressing and Parental Cells.

Compd	R^1	R^2	Scaffold	GI_{50} ABCG2 ± SD [µM] [a]	GI_{50} Parental ± SD [µM] [a]	Therapeutic ratio[d]
12	3-Pyr	3- NO_2	A	70.8 ± 23.2	64.6 ± 20.4	615
14	3-Pyr	4- NO_2	A	73.3 ± 17.1	74.1 ± 28.0	1140
16	3-Pyr	3-CN	A	75.3 ± 18.8	90.7 ± 20.2	697
17	4-Pyr	3-CN	A	88.1 ± 8.6	112 ± 20	657
18	3-Pyr	4-CN	A	79.4 ± 4.6	104 ± 8	241
26	4-Pyr	3-CF_3	A	12.6 ± 2.8	12.3 ± 3.3	58.3
27	4-Pyr	4-CF_3	A	117 ± 41	166 ± 38	240
28	4-Pyr	3-CF_3,4-OMe	A	2.88 ± 0.10	2.46 ± 0.08	19.7
29	3-Pyr	3-F	A	46.8 ± 4.7	100 ± 16	300
31	3-Pyr	3-$N(Me)_2$	A	10.0 ± 0.7	14.1 ± 0.6	8.33
32	4-Pyr	3-OH	A	9.22 ± 0.32	12.4 ± 0.2	8.62
33	4-Pyr	4-OH	A	55.0 ± 12.7	120.2 ± 7.0	12.9
42	4-Pyr	3-CN	B	6.92 ± 2.04	9.33 ± 0.60	52.4
46	Ph	4-CN	B	17.8 ± 0.1	28.4 ± 2.3	139
47	Ph	3-NO_2,4-OH	B	49.0 ± 3.2	57.5 ± 1.2	496
48	Ph	H	B	107 ± 4	136 ± 35	165
49	Ph	4-CN	A	10.4 ± 2.0	14.2 ± 2.0	146
51[b]	Ph	3-NO_2,4-OH	A	52.4 ± 1.7	152 ± 43	647
52[b]	Ph	4-OH	A	14.6 ± 1.7	22.6 ± 3.7	69.2
53[b]	Ph	3-F	A	18.0 ± 1.9	27.5 ± 0.7	49.6
54[b]	Ph	H	A	26.6 ± 1.2	26.0 ± 2.1	30.1
55				12.6 ± 0.6	12.5 ± 0.8	48.9
MeOH/DMSO				96.1[c] ± 13	125[c] ± 16	

[a]: Concentration accomplishing 50% of the maximal inhibition of cell proliferation with MDCK II BCRP and parental cells, respectively. The data was obtained from at least two independent experiments as mean values.
[b]: Compound was synthesized before. [30]
[c]: Positive control of the cytotoxicity from dilution with DMSO/MeOH without compound.
[d]: The therapeutic ratio (TR) was calculated as the ratio of GI_{50} and IC_{50} values for the MDCK II BCRP cells.

Table 4. EC_{50} Values of Selected Compounds in the ATPase Activity Assay. All Values are Relative Vanadate-sensitive ATPase Activities in Relation to the Basal Activity, which is Set to 100%

Comp.	EC_{50} [nM]	V_{max} [% of control]
11	676	119
12	21	154
13	4	185
14	9	164
15	1530	115
16	350	151
17	16	178
18	4	137
20	50	137
21	42	132
22	70	137
23	79	152
25	10	150
29	58	140
36	7	151
39	1540	40 *
42	22	133
43	82	144
44	85	146
45	2080	134
46	2460	140
47	1800	154
48	no effect	100
49	15	145
51	20	135
53	131	142
Quercetin	278	177
biphasic	K_M [nM]	K_i [nM]
26	9	28000 155
27	2	27000 152

*inhibiting compound

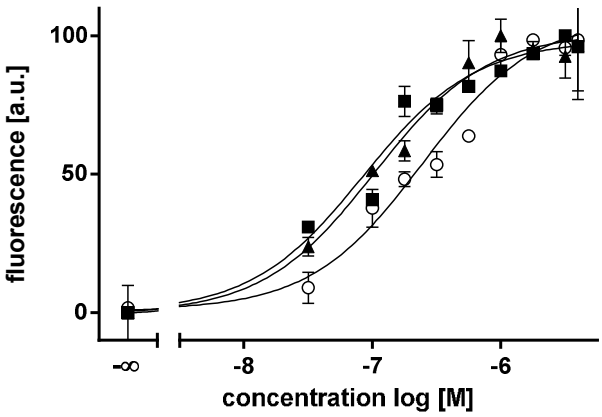

Figure 1. Concentration-response curve of compound **14** (■, IC_{50} = 64.1 nM) and **47** (▲, IC_{50} = 98.8 nM) in a Hoechst 33342 accumulation assay with compound **55** (○, IC_{50} = 227 nM) as reference, using the ABCG2 overexpressing MDCK II cell line.

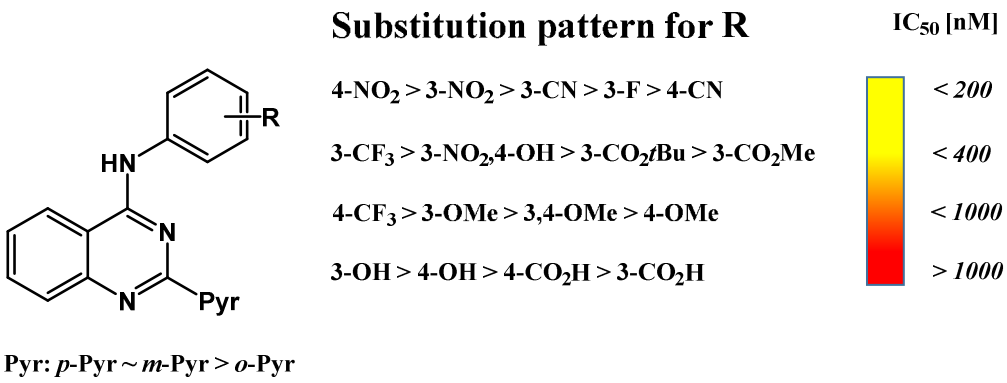

Figure 2: SAR of some substitution patterns used in derivatives with scaffold A. IC_{50} range corresponds to given residue containing *p*-pyridyl or *m*-pyridyl that were found to be about equally active. Regarding compounds containing scaffold B the same ranking and similar IC_{50} values were obtained in comparison to scaffold A.

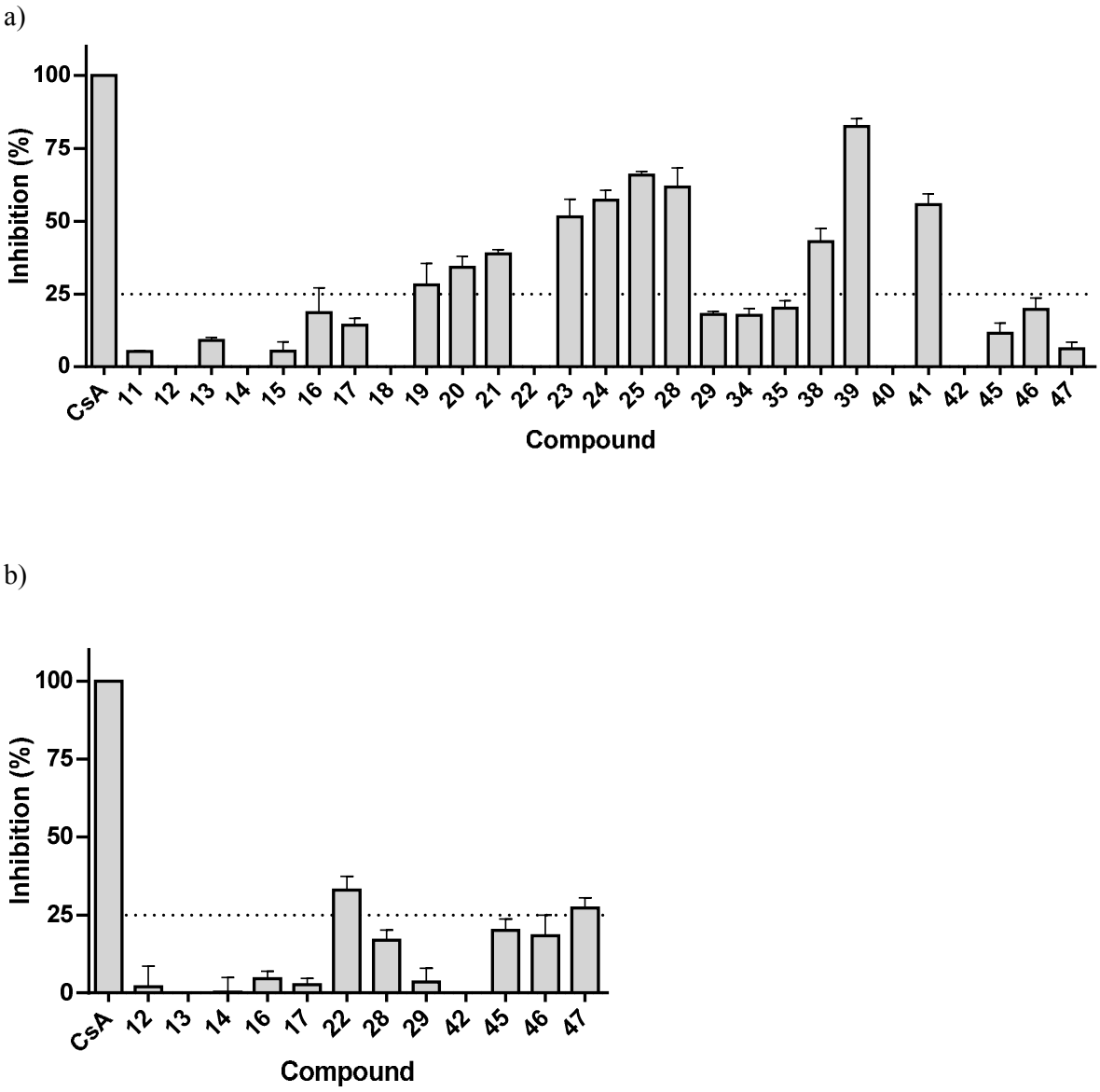

Figure 3. Inhibitory effect of screened compounds toward ABCB1 overexpressing cell line A2780adr (a) and ABCC1 overexpressing cell line H69AR (b) in a calcein AM assay at a concentration of 10 µM. Cyclosporine A (CsA) was used as positive control, indicating complete inhibition. The length of the bars represents the inhibition compared to the positive control in percent. For each compound, three independent experiments were performed and the standard deviation expressed as error bars.

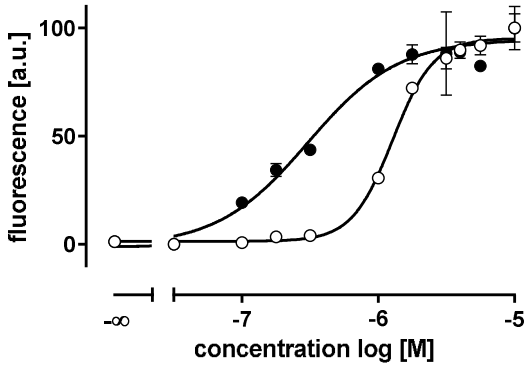

Figure 4. Concentration-response curve of compound **39** (●, IC_{50} = 0.334 μM) in a calcein AM assay with cyclosporine A (○, IC_{50} = 1.21 μM) as reference, using the ABCB1 overexpressing cell line A2780adr. Results were obtained in at least three independent experiments and the standard deviation is expressed by error bars.

a)

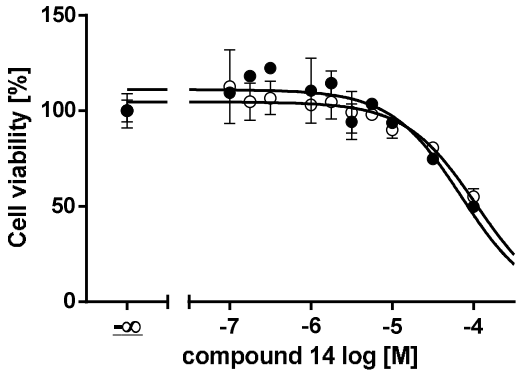

b)

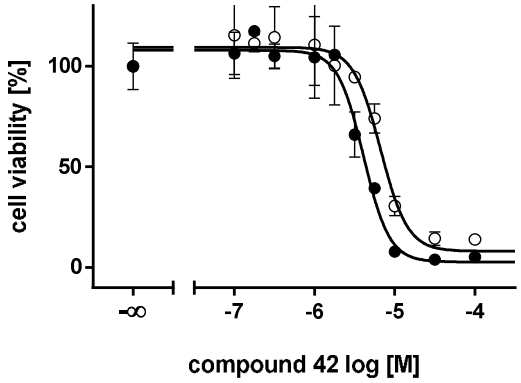

Figure 5. Representative examples of MTT viability assays of compounds **14** and **42** with low and higher cytotoxicity using the MDCK II ABCG2 overexpressing (closed circle) and parental MDCK II cell line (open circle). There is no significant difference in the intrinsic toxicities comparing the parental and ABCG2 expressing cells.

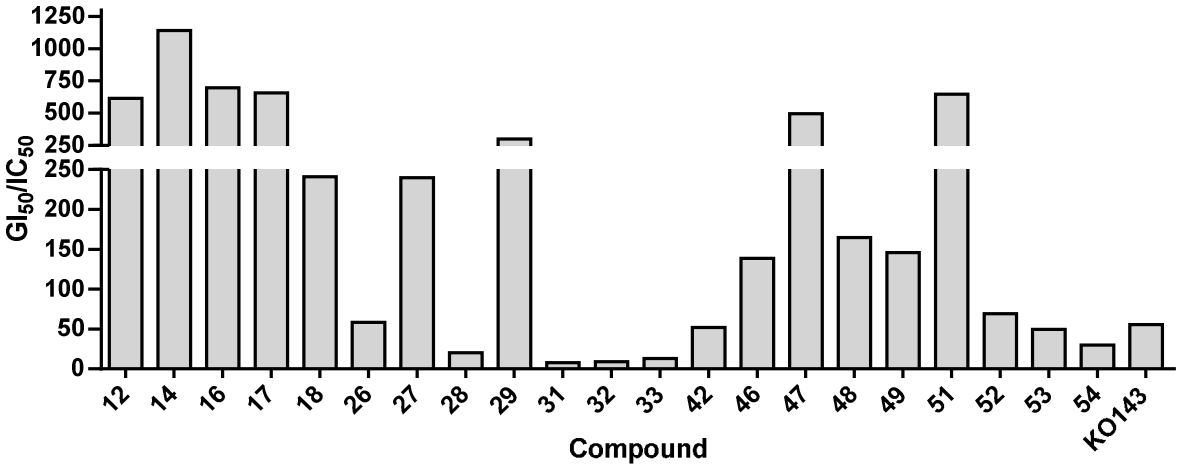

Figure 6. Therapeutic ratios of selected compounds, calculated from the ratio of GI_{50} to IC_{50} derived from MTT viability assay and Hoechst 33342 accumulation assay, respectively. The highest score was obtained for compound **14** (**GI_{50}/IC_{50}** = 1140), while the reference compound **55** yielded GI_{50}/IC_{50} = 55.5.

a)

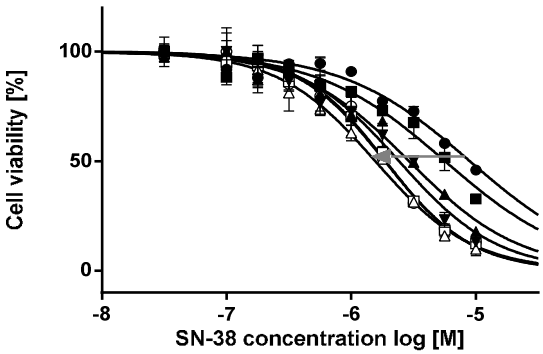
Cell viability [%]
100
50
0
-8
-7
-6
-5
SN-38 concentration log [M]

b)

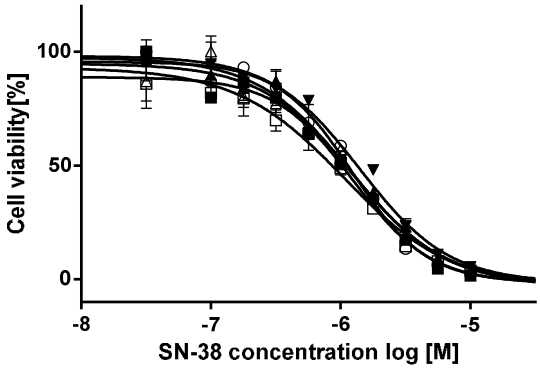
Cell viability[%]
100
50
0
-8
-7
-6
-5
SN-38 concentration log [M]

c)

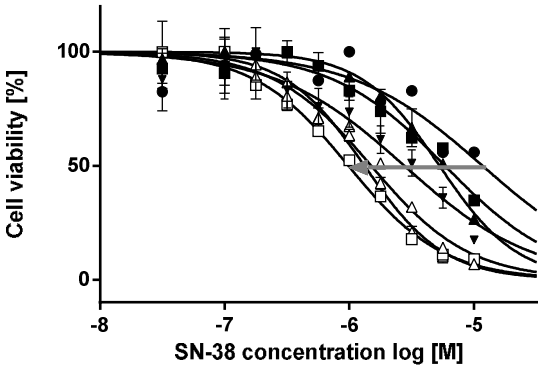
Cell viability [%]
100
50
0
-8
-7
-6
-5
SN-38 concentration log [M]

d)

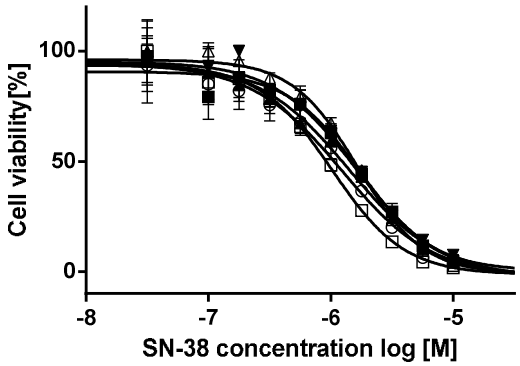
Cell viability[%]
100
50
0
-8
-7
-6
-5
SN-38 concentration log [M]

e)

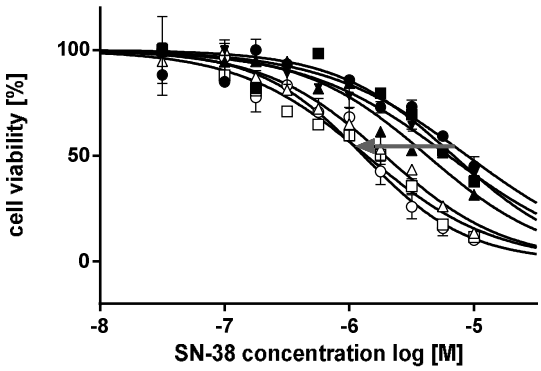

f)

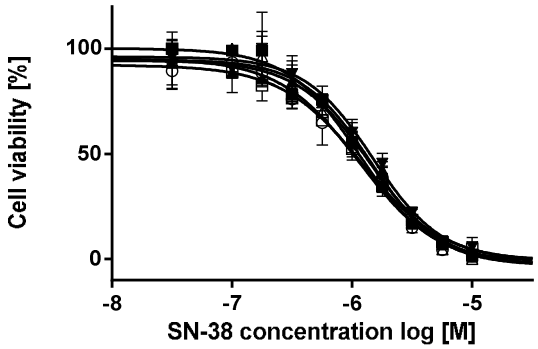

Figure 7. MTT assay to determine the ability of compounds **14** (a, b), **16** (c, d) and **47** (e, f) to reverse the resistance against the cytostatic SN-38, using the ABCG2 overexpressing cell line (a, c and e) and parental MDCK II cells (b, d, f). The grey arrow indicates the increasing sensitization of the ABCG2 overexpressing cells with higher compound concentrations. The following concentrations were used: control (closed circle), 0.01 µM (closed square), 0.03 µM (closed triangle), 0.1 µM (closed down triangle), 1 µM (open triangle), 5 µM (open square), parental cell line (open circle). At a compound concentration of 1 µM, full reversal is achieved, indicated by a similar pGI_{50} as the parental cells.

a)

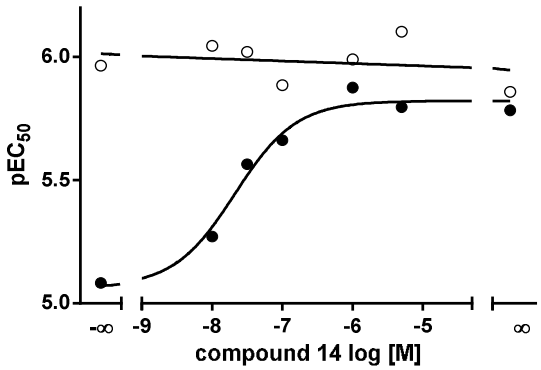

b)

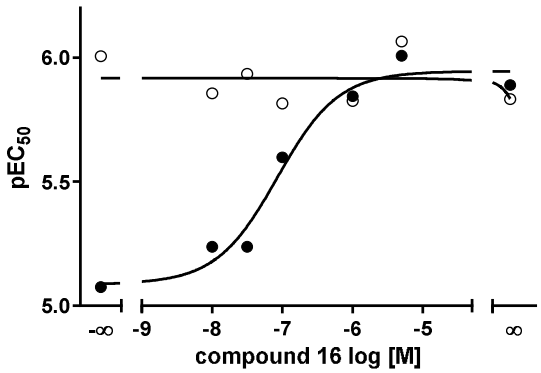

c)

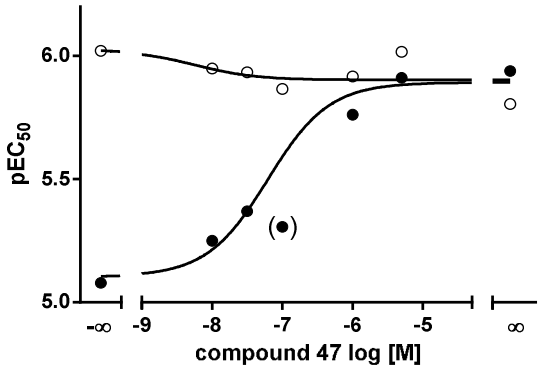

Figure 8. Nonlinear regression of the pGI_{50} values determined in the MDR reversal assay (Figure 7 a, c and e) against the corresponding concentrations of compounds **14**, **16** and **47**. pEC_{50} is the concentration that reduces resistance of the ABCG2 overexpressing cells to 50 percent. The following EC_{50} values were calculated: 21.2 nM (**14**), 85.0 nM (**16**) and 62.3 nM

(**47**). The pGI_{50} values of the parental cells determined in an analogous assay (Figure 7 b, d and f) are depicted by open circles. The point in parenthesis at 0.1 μM in (c) was excluded.

a)

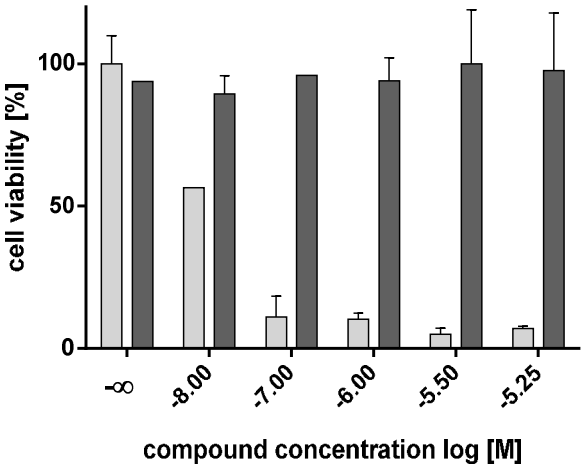

b)

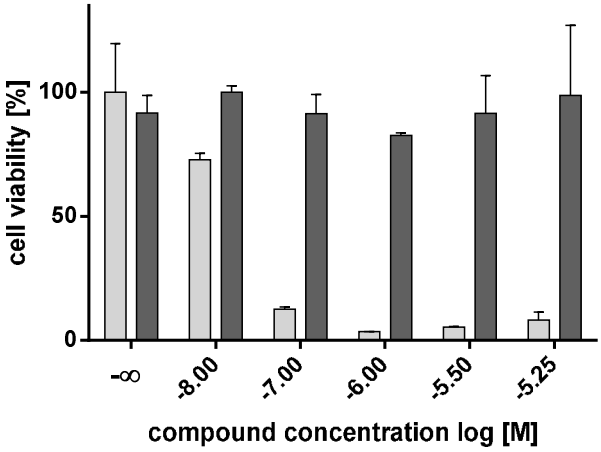

Figure 9. MDR reversal assay of compound **14** (a, EC_{50}: 12.6 nM) and **47** (b, EC_{50}: 22.0 nM), demonstrating the ability to reverse the MDR toward the cytostatic MX, using ABCG2 overexpressing cell line MDCK II. The bars represent the cell viability at a given modulator concentration in the presence (light grey) and absence (dark grey) of 5 μM MX. The control shows cell viability of cells without modulator in the presence and absence of 5 μM MX. Standard deviation is expressed by error bars.

a)

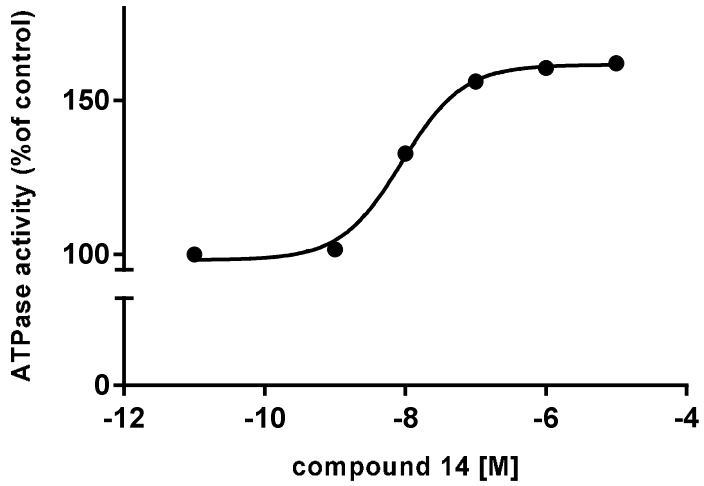
ATPase activity (%of control)
150
100
0
-12
-10
-8
-6
-4
compound 14 [M]

b)

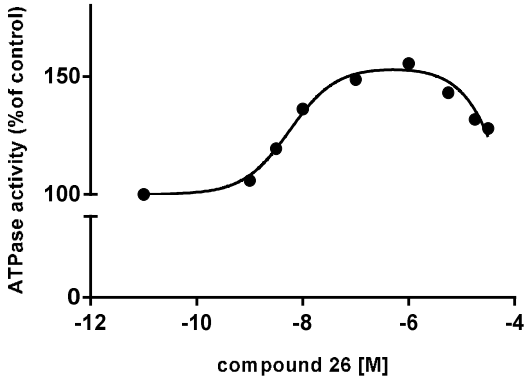
ATPase activity (%of control)
150
100
0
-12
-10
-8
-6
-4
compound 26 [M]

c)

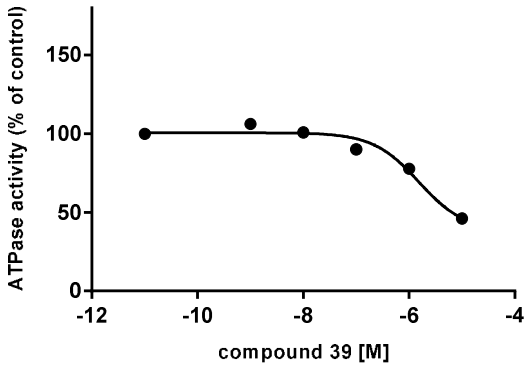

d)

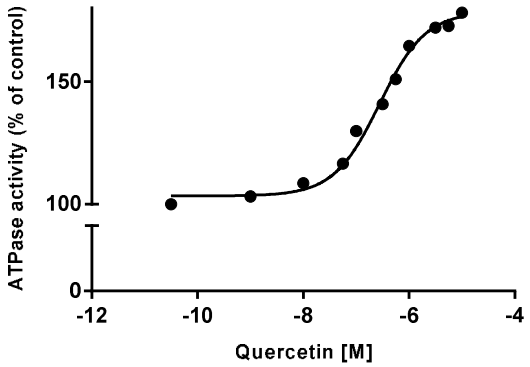

Figure 10. Concentration-response curves for compounds **14**, **26**, **39** and **Quercetin** in the ATPase assay. All values are relative vanadate-sensitive ATPase activities in relation to the basal activity, which is set to 100%.

a)

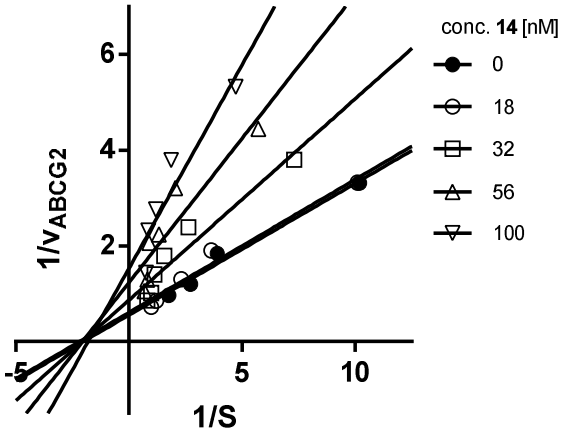
conc. 14 [nM]
0
18
32
56
100
1/v ABCG2
1/S
6
4
2
-5
5
10

b)

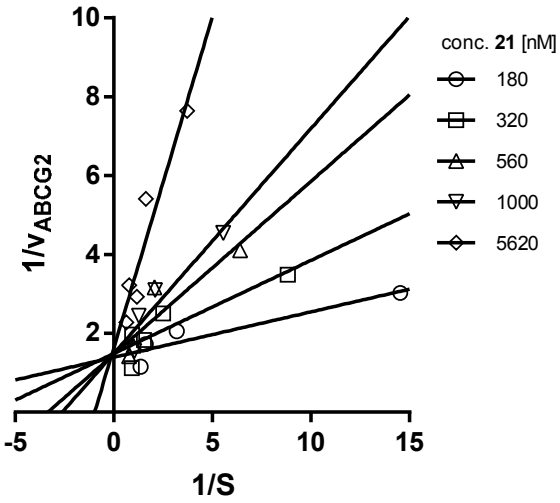
conc. 21 [nM]
180
320
560
1000
5620
1/v ABCG2
1/S
10
8
6
4
2
-5
0
5
10
15

c)

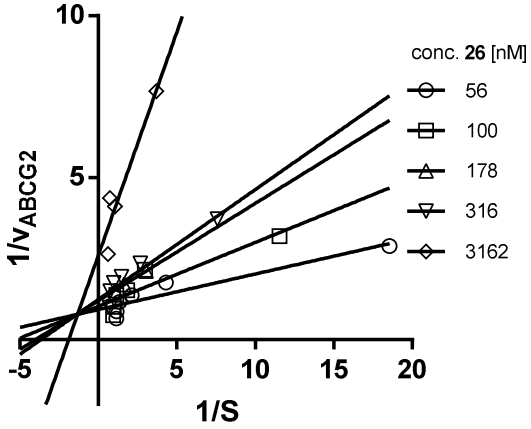
conc. 26 [nM]
56
100
178
316
3162
1/v ABCG2
1/S
10
5
-5
5
10
15
20

d)

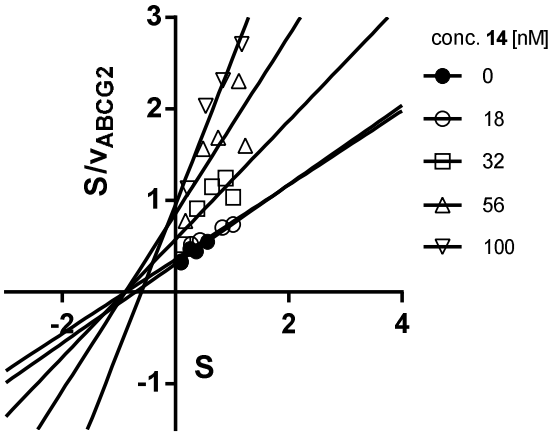
S/v ABCG2
S
conc. 14 [nM]
0
18
32
56
100

e)

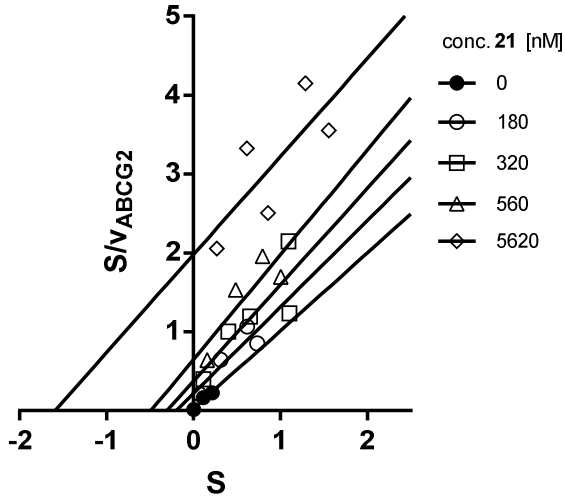
S/v ABCG2
S
conc. 21 [nM]
0
180
320
560
5620

f)

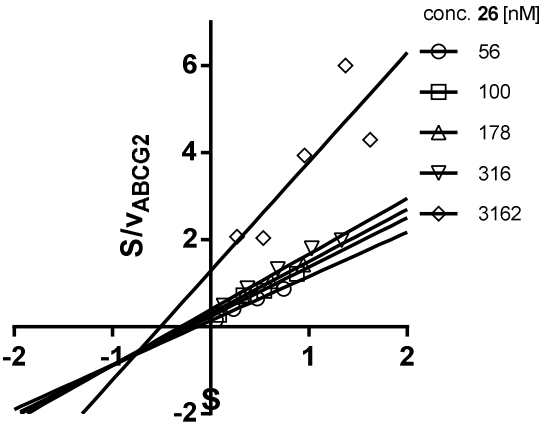
S/v ABCG2
S
conc. 26 [nM]
56
100
178
316
3162

g)

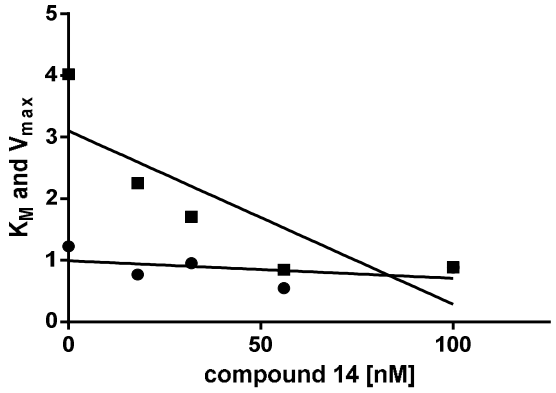

h)

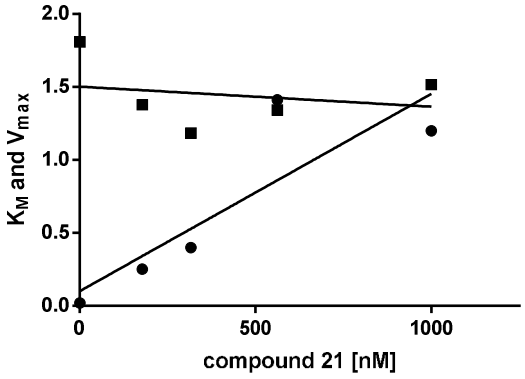

i)

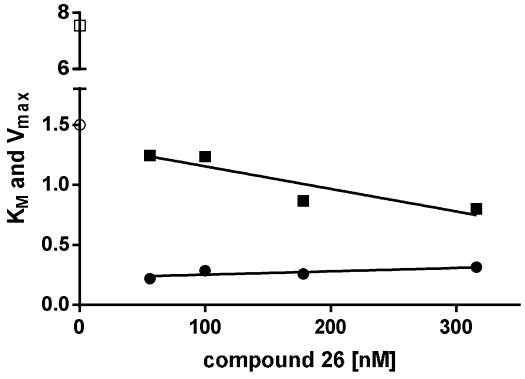

Figure 11. Lineweaver–Burk plots for compounds **14** (a), **21** (b) and **26** (c) at various concentrations together with the ABCG2 substrate Hoechst 33342. Hanes-Woolf plots at various concentrations of Hoechst 33342 for compounds **14** (d), **21** (e) and **26** (f). Plot of the

Michaelis-Menten constant K_M (closed circle) and the maximum velocity V_{max} (closed square) derived from the analysis according to Cornish-Bowden against the corresponding compound concentration (g, h, i). Here excluded values are depicted by the corresponding open symbols.

Table of Contents Graphic